

NAG3-673

P64

Nonlinear Binary-Mode Interactions in a
Developing Mixing Layer

by

D. E. Nikitopoulos and J. T. C. Liu

The Division of Engineering

Brown University

Providence, Rhode Island 02912, U.S.A.

RECEIVED
A.I.M.A.
MAY 16 1987
T.I.S. LIBRARY

LEWIS-GRANT

7N-34

79423 CR

ABSTRACT

In this paper we present the formulation and results of two-wave interactions in a spatially developing shear layer, directed at understanding and interpreting the physical mechanisms that underlie the results of quantitative observation. Our study confirms the existence of Kelly's mechanism that augments the growth of a subharmonic disturbance by extracting energy from its fundamental or vice versa. This mechanism is shown to be strongest in the region where the fundamental begins to return energy to the mean flow and the two wave modes are of comparable energy levels. It is found that the initial conditions and especially the initial phase angle between the two disturbances play a very significant role in the modal development and that of the shear layer itself. A doubling of the mean flow is shown to take place; the two successive plateaus in its growth are attributed to the peaking of the fundamental and subharmonic amplitudes.

Submitted to JFM April 1986

N87-70438

Unclass
0079423

00/34

(NASA-CR-181033) NONLINEAR BINARY-MODE
INTERACTIONS IN A DEVELOPING MIXING LAYER
(Brown Univ.) 64 p Avail: NTIS

1. INTRODUCTION

Sato (1959) appears to have been the first to observe what was then a rather curious development of a subharmonic disturbance in the transition region of a separated plane shear layer. This is subsequently brought to light further by the experiments of Wille (1963), Freymuth (1966), Browand (1966), Miksad (1972, 1973), Winant and Browand (1974) and more recently Ho and Huang (1982). A theoretical explanation of conditions favorable for the subharmonic development in free shear layers was given by Kelly (1967). These conditions include a finite threshold for the fundamental disturbance and more importantly, Kelly's (1967) work implies that a "favorable" phase relation must exist between the fundamental and its subharmonic. Although Kelly's mechanism was arrived via weak nonlinear arguments that necessarily involve small amplification rates, the basic physical consequences, rather than the details, have much more universality than the original framework (Liu 1981). On the other hand, for real developing shear layers the disturbance growth rates are anything but small in the incipient transition region as experiments indicate (see, for instance, Ho and Huang 1982).

Quantitative measurements of the disturbance amplitudes indicate that the subharmonic, at half the frequency of the fundamental, peaks further downstream than the fundamental in a spatially developing shear layer (Ho and Huang 1982). Each individual component, in fact, undergoes a life cycle of amplification and decay. Although the peaks in amplitude do not

overlap, there is a significant spatial, finite-amplitude region of overlap between the fundamental mode and its subharmonic. The switching in modal content of the disturbances is revealed by the quantitative amplitude measurements (Ho and Huang 1982) to be a gradual process rather than an abrupt one as might have been suggested by visual observations of dye streaks alone. Of course, we were already cautioned by the work of Williams and Hama (1980). They showed that a linear superposition of constant amplitude fundamental and subharmonic wave functions in a shear layer could produce interference effects that lead to dye streak accumulation suggesting the switch in modal content, when in fact, each of the wave components are quite distinct.

In this paper we shall present the formulation and results for mode interactions in a spatially developing shear layer, directed at understanding and interpreting the physical mechanisms that underlie the results of quantitative observations. The basic framework in this consideration is an explicit account of the energy budget of each individual disturbance component as well as that of the mean flow (Nikitopoulos 1982, Liu and Nikitopoulos 1982). This necessitates the accounting of the rate of energy exchange between the various scales of motion. While the rate of energy exchange between each disturbance mode and the mean flow is fairly well understood (the "production" mechanism), the rate of energy exchange between modes might still be somewhat novel. Although directed at first towards the understanding of the interaction between the fundamental and its harmonic but which is

also appropriate for the subharmonic problem, Stuart (1962) split the flow quantity for an ensemble of disturbances into odd and even modes. The rate of energy transfer from the even to the odd modes is then $\overline{u_i' u_j' \partial u_i'' / \partial x_j}$, where $()'$ denotes odd and $()''$ denotes even modes and the average is taken over the largest periodicity of the disturbances. This is interpreted as the work done by the stresses of the odd modes against the rates of strain of the even modes. The mechanism that we attribute to Kelly (1967) is clear from the present energy transfer consideration in that the phase relation between the stresses of the odd modes and the appropriate rates of strain of the even modes determines the direction of energy transfer and that the mode amplitudes determine the strength of this transfer. However, for a real laboratory shear layer, the fundamental component is one which has the largest initial amplification rate resulting in rather strong interactions with the mean motion. The subharmonic component evolves into a similar situation in a spatial region for which its local amplification rate also reaches a "momentary" maximum. These interactions with the mean flow scale with an amplitude to the second power via the Reynolds stresses, whereas the mode interactions would scale as a typical amplitude to the third power from the above discussion of the rate of energy transfer. Thus, in a developing shear layer, the individual modal production rate from the mean flow is anticipated to be the dominant mechanism for disturbance evolution. In this case, the dominant mode interactions would be the implicit nonlinear interactions via the mean flow rather than by the more explicit

direct energy transfer between the modes. The latter mechanism is, however, most important in affecting the details of the spatial distribution of the amplitudes.

2. CONSERVATION EQUATIONS

In a laboratory observations of the transition region in shear layers there usually exist modes other than the fundamental and the subharmonic including perhaps initially weak fine-grained turbulence. The latter coexisting with monochromatic coherent disturbances, has been the subject of discussion elsewhere (see, for instance, Liu 1981) and will be excluded from consideration here. We shall concentrate on the understanding of coherent mode interactions in an otherwise laminar viscous shear flow. We shall start from the Navier-Stokes equations for an incompressible fluid and split the total flow quantity into that for the mean motion Q and the overall disturbance \tilde{q} consisting of $(q' + q'')$, where q' denotes the odd mode and q'' denotes the even mode (Stuart 1962). The mean flow momentum and continuity equations are obtained following this Reynolds' splitting and averaging,

$$\frac{DU_i}{Dt} = - \frac{\partial(\tilde{u}_i \tilde{u}_j)}{\partial x_j} - \frac{\partial P}{\partial x_i} + \frac{1}{Re} \frac{\partial^2 U_i}{\partial x_i \partial x_j} \quad (2.1)$$

$$\frac{\partial U_i}{\partial x_i} = 0 \quad (2.2)$$

where appropriate (constant) length and velocity scales are used to make the equations dimensionless, U_i and P are the mean flow velocity and pressure respectively, \tilde{u}_i the total disturbance velocity, x_i the spatial coordinates, t the time and Re the Reynolds number. The bar over the substantial derivative indicates that the derivative is taken following the mean flow. The corresponding total disturbance momentum and continuity equations are

$$\frac{D\tilde{u}_i}{Dt} + \tilde{u}_j \frac{\partial \tilde{u}_i}{\partial x_j} = - \frac{\partial \tilde{P}}{\partial x_i} + \frac{1}{Re} \frac{\partial^2 \tilde{u}_i}{\partial x_i \partial x_j} - \frac{\partial (\tilde{u}_i \tilde{u}_j - \overline{\tilde{u}_i \tilde{u}_j})}{\partial x_j} \quad (2.3)$$

$$\frac{\partial \tilde{u}_i}{\partial x_j} = 0 \quad (2.4)$$

where \tilde{p} is the total disturbance pressure. Equations (2.1) - (2.4) are identical in form to the Reynolds system. Following Stuart (1962), the total disturbance is split into the odd and even modes, $\tilde{u}_i = u'_i + u''_i$. The linear terms in (2-3) and (2-4) are correspondingly split and would retain their respective interpretations in the individual conservations for the odd and even modes. The nonlinear effect, through $\partial(\tilde{u}_i \tilde{u}_j - \overline{\tilde{u}_i \tilde{u}_j})/\partial x_j$, deserves further comment. The results from the mode splitting give rise to the nonlinear term $\partial(u'_j u''_i + u''_j u'_i)/\partial x_j$ for the odd-mode momentum equation, with $\overline{u'_i u''_j} = 0$. The even-mode momentum equation would obtain the even contributions from $\partial(u'_i u'_j - \overline{u'_i u'_j})/\partial x_j$ and $\partial(u''_i u''_j - \overline{u''_i u''_j})/\partial x_j$. However, the mean

kinetic energy equations for the odd and even modes would be coupled through the mode interaction mechanism $\overline{u'_i u'_j \partial u''_i / \partial x_j}$ as follows.

For purposes of obtaining the "amplitude" equations at a later stage, we first obtain the energy equations for the various scales of motion as follows:

Mean motion

$$\begin{aligned} \frac{D}{Dt} \left(\frac{U_i^2}{2} \right) = & - (\overline{u'_i u'_j} - \overline{u''_i u''_j}) \left(\frac{\partial U_i}{\partial x_j} \right) - \frac{1}{Re} \left(\frac{\partial U_i}{\partial x_j} \right)^2 + \\ & - (\text{production}) \qquad \qquad \text{dissipation} \\ & + \frac{\partial}{\partial x_j} \left[\frac{1}{Re} \frac{\partial}{\partial x_j} \left(\frac{U_i^2}{2} \right) - P U_j - U_i (\overline{u'_i u'_j} + \overline{u''_i u''_j}) \right]. \\ & \qquad \qquad \qquad \text{"diffusion"} \end{aligned} \tag{2.5}$$

Odd modes

$$\begin{aligned} \overline{\frac{D}{Dt} \left(\frac{u_i'^2}{2} \right)} = & (\overline{-u'_i u'_j}) \frac{\partial U_i}{\partial x_j} - \overline{u'_i u'_j \frac{\partial u''_i}{\partial x_j}} - \frac{1}{Re} \overline{\left[\frac{\partial u'_i}{\partial x_j} \right]^2} \\ & \text{production} \quad \left(\begin{array}{c} \text{mode} \\ \text{interaction} \end{array} \right) \text{dissipation} \\ & + \frac{\partial}{\partial x_j} \left[\frac{1}{Re} \frac{\partial}{\partial x_j} \left(\frac{u_i'^2}{2} \right) - \overline{p' u'_j} - \overline{u''_j \frac{u_i'^2}{2}} \right] \\ & \qquad \qquad \qquad \text{"diffusion"} \end{aligned} \tag{2.6}$$

Even modes

$$\begin{aligned}
 \frac{\overline{D}}{Dt} \left(\frac{\overline{u_i''^2}}{2} \right) = & \underbrace{\left(- \overline{u_i'' u_j''} \right) \frac{\partial U_i}{\partial x_j}}_{\text{production}} + \underbrace{\overline{u_i' u_j'} \frac{\partial u_i''}{\partial x_j}}_{\text{mode interaction}} - \underbrace{\frac{1}{Re} \left[\overline{\frac{\partial u_i''}{\partial x_j}}^2 \right]}_{\text{dissipation}} \\
 & + \underbrace{\frac{\partial}{\partial x_j} \left[\frac{1}{Re} \frac{\partial}{\partial x_j} \left(\frac{\overline{u_i''^2}}{2} \right) - \overline{p'' u_j''} - \overline{u_j''} \frac{\overline{u_i''^2}}{2} - \overline{u_i'' u_j' u_j'} \right]}_{\text{"diffusion"}}. \quad (2.7)
 \end{aligned}$$

The usual Reynolds' time average has been used and we note that the products $\overline{u_i' u_j''}$ are uncorrelated but that the triple products such as $\overline{u_i' u_j' \partial u_i'' / \partial x_j}$ are. These latter products are interpreted as the work done by the stresses of the odd modes against the appropriate rates of strain of the even modes and are responsible for the net energy transfer between the odd and even modes. Both the even and odd modes have their respective production mechanism, responsible for the extraction of energy from or a return of energy to the mean shearing motion. The remaining mechanisms include the rate of viscous dissipation of the various scales of motion and of "diffusion" by viscosity and by the fluctuating motions.

The discussion is so far general in that we have not specified whether the problem is spatial or temporal. For the

spatial problem the Reynolds average is then the time average, the periodicity is in time and the amplitudes (or "envelopes") of the fluctuations grow and decay spatially. In the temporal problem, the Reynolds average is spatial connected with the spatial periodicity and the amplitudes of fluctuations evolve in time. In the following we shall study the observed or observable spatially developing shear layer for which the fluctuations have periodicity in time. In this case the odd modes consist of frequencies $\beta, 3\beta, \dots, (2n - 1)\beta$ and the even modes consist of $2\beta, 4\beta, \dots, 2n\beta$, where n is an integer. Thus mode $u''_i(2\beta)$ would correspond to, say, the fundamental component and $u'_i(\beta)$ would then be its subharmonic. In Section 3 we shall consider the nonlinear interactions between modes 2β and β in a developing shear layer, the simplest case of mode interactions.

3. TWO-MODE INTERACTIONS

In this section we shall apply the general framework obtained previously to study the two mode interaction problem. The even mode, u'' , would thus be interpreted as that of the fundamental mode with frequency 2β ; the odd mode, u' , would be its subharmonic of frequency β . For the objective of obtaining the "amplitude" or "envelope" equations, in terms of the observable kinetic energy content across the shear layer for each mode, we begin with (2.5) - (2.7) for a thin shear layer for which the boundary layer type of approximations hold for the mean quantities. The schematical representation of the shear layer is shown in Figure 1. The simplified kinetic energy equations are

then integrated across the plane shear layer to give

$$\frac{1}{2} \frac{d}{dx} \left[\int_{-\infty}^0 U(U^2 - U_{-\infty}^2) dz + \int_0^{\infty} U(U^2 - U_{+\infty}^2) dz \right] = - \int_{-\infty}^{\infty} (\overline{u'w'} - \overline{u''w''}) \frac{\partial U}{\partial z} dz - \overline{\phi}, \quad (3.1)$$

$$\begin{aligned} \frac{1}{2} \frac{d}{dx} \int_{-\infty}^{\infty} U(\overline{u'^2 + w'^2}) dz &= \int_{-\infty}^{\infty} (\overline{-u'w'}) \frac{\partial U}{\partial z} dz - \\ &- \int_{-\infty}^{\infty} \left[\overline{u'^2 \frac{\partial u''}{\partial x}} + \overline{u'w' \left(\frac{\partial u''}{\partial z} + \frac{\partial w''}{\partial x} \right)} + \overline{w'^2 \frac{\partial w''}{\partial z}} \right] dz - \overline{\phi'} \end{aligned} \quad (3.2)$$

$$\begin{aligned} \frac{1}{2} \frac{d}{dx} \int_{-\infty}^{\infty} U(\overline{u''^2 + w''^2}) dz &= \int_{-\infty}^{\infty} (\overline{-u''w''}) \frac{\partial U}{\partial z} dz + \\ &+ \int_{-\infty}^{\infty} \left[\overline{u'^2 \frac{\partial u''}{\partial x}} + \overline{u'w' \left(\frac{\partial u''}{\partial z} + \frac{\partial w''}{\partial x} \right)} + \overline{w'^2 \frac{\partial w''}{\partial z}} \right] dz - \overline{\phi''}, \end{aligned} \quad (3.3)$$

where x is the streamwise coordinate measured from the start of the mixing layer, z is the vertical coordinate measured from the center of the mixing layer, u, w are the x, z fluctuation velocities, U is the mean velocity with $\pm\infty$ denoting the upper

(say, slower) and lower free streams, respectively; $\bar{\phi}$ is the integral of mean flow viscous dissipation and the lower case $\bar{\phi}'$ and $\bar{\phi}''$ represent the corresponding dissipation rates of the fluctuations. Equations (3.1) - (3.3), where two-dimensional wavy disturbances in a two-dimensional mean flow have been assumed, form the basis for obtaining the evolution equations for the measurable energy content of the disturbances across the shear layer.

(a) Shape assumptions

Following earlier work (see, for instance, Stuart 1958; Liu 1981), the "closure" for the disturbances are obtained by assuming the separable form of the product of an unknown finite amplitude $A_n(x)$ with a vertical distribution function given by the local-linear stability theory,

$$\begin{pmatrix} u' \\ w' \end{pmatrix} = A_1(x) \left[\begin{pmatrix} \phi_1' e^{-i\beta t} \\ -i\alpha_1 \phi_1 e^{-i\beta t} \end{pmatrix} + \begin{pmatrix} \text{c.c.} \\ \text{c.c.} \end{pmatrix} \right] \quad (\text{Subharmonic})$$

$$\begin{pmatrix} u'' \\ w'' \end{pmatrix} = A_2(x) \left[\begin{pmatrix} \phi_2' e^{-2i\beta t - i\theta_2} \\ -i\alpha_2 \phi_2 e^{-2i\beta t - i\theta_2} \end{pmatrix} + \begin{pmatrix} \text{c.c.} \\ \text{c.c.} \end{pmatrix} \right], \quad (\text{Fundamental})$$

where ϕ_i here denotes the eigenfunction of the local linear theory and is a function of the rescaled vertical variable $\eta = z/\delta(x)$; $\delta(x)$ is a length scale of the mean flow yet to be identified and $()'$ denotes differentiation with respect

to η ; $\beta = 2\pi f\delta(x)/\bar{U}$ is the dimensionless local (Strouhal) frequency, f is the physical frequency and $\bar{U} = (U_{\infty} + U_{-\infty})/2$, the local wave-numbers α are also scaled by $\delta(x)$. The angle θ_2 is the relative phase between the fundamental component (2β) and its subharmonic (β) and c.c. denotes the complex conjugate. The velocities and lengths are considered to be made dimensionless by \bar{U} and δ_0 (so that $\delta(0) = 1$), and time by δ_0/\bar{U} . These two-dimensional disturbances have their vorticity axis perpendicular to the direction of the free streams.

As far as the mean-flow is concerned we will assume a hyperbolic tangent type profile, which has experimentally proven to be very close to reality away from the splitter plate into the developed mixing-layer region (Wynanski et al. 1979; Fiedler 1980; Ho and Huang 1982),

$$U = 1 - R \tanh \eta,$$

where

$$R = (U_{-\infty} - U_{+\infty}) / (U_{-\infty} + U_{+\infty})$$

is the velocity ratio of the shear layer. Since $\eta = z/\delta(x)$, it is now understood that $\delta(x)$ is the half-maximum slope thickness of the shear layer. This characterizes the mean motion and must be jointly determined with the amplitudes $A_1(x)$ of the finite disturbances.

Both shape functions ϕ_1 and ϕ_2 are taken to be governed locally by the Rayleigh equation (see Liu and Merkin 1976)

according to linear stability analysis with the appropriate boundary conditions,

$$(U-c)(\phi'' - \alpha^2 \phi) - \phi U'' = 0 ,$$

where c is the phase velocity scaled by the mean velocity \bar{U} of the two free streams. This, of course, is an approximation since the viscous terms have been dropped. We deal here with an inflectional mean velocity profile which is dynamically unstable and thus the inviscid equation suffices. The Rayleigh equation yields solutions that correspond to amplified disturbances up to the point $\beta = 1$ of neutral stability. In the neighborhood of this point and for values of β larger than 1 (corresponding to damped disturbances) the equation becomes singular. In order to obtain solutions in the locally damped region use is made of a complex integration contour scheme first discussed by Lin (1955) and successfully applied by Mack (1965) and Zaat (1958) for the case of a boundary layer. The amplification rates $-\alpha_1$ versus β are shown in Figure 2, providing the necessary "state" diagram for initial disturbances in the subsequent nonlinear problem.

The eigenfunction ϕ_1 and ϕ_2 are normalized so as to render $|A_1(x)|^2$ and $|A_2(x)|^2$ to corresponding energy densities of each mode of the finite disturbances such that the mode energy contents across the shear layer are

$$E_1(x) = \frac{1}{2} \int_{-\infty}^{+\infty} (\overline{u'^2 + w'^2}) dy = |A_1(x)|^2 \delta(x),$$

$$E_2(x) = \frac{1}{2} \int_{-\infty}^{+\infty} (\overline{u''^2 + w''^2}) dy = |A_2(x)|^2 \delta(x).$$

This is similar to Ho and Huang's (1982) $E(f)$, except that their energy content refers to the contribution by u alone. The normalization of the local eigen-functions allows us to relate the energy content to the amplitude.

(b) The nonlinear interaction problem

After substituting the shape assumptions into (3.1) - (3.3) we then obtain three first-order nonlinear differential equations describing the streamwise evolution of δ, E_1 and E_2 (or $\delta, |A_1|^2$ and $|A_2|^2$):

Mean flow

$$I_m \frac{d\delta}{dx} = [I_{rs2}(\delta)E_2 + I_{rs1}(\delta)E_1]/\delta + \frac{1}{Re} I_d/\delta, \quad (3.4)$$

Subharmonic

$$\overline{I_1(\delta)} \frac{dE_1}{dx} = I_{rs1}(\delta)E_1/\delta - I_{21}(\delta)E_1E_2^{1/2}/\delta^{3/2} - \frac{1}{Re} I_{d1}(\delta)E_1/\delta^2, \quad (3.5)$$

Fundamental

$$\overline{I_2(\delta)} \frac{dE_2}{dx} = I_{rs2}(\delta)E_2/\delta + I_{21}(\delta)E_1E_2^{1/2}/\delta^{3/2} - \frac{1}{Re} I_{d2}(\delta)E_2/\delta^2. \quad (3.6)$$

Equations (3.4) - (3.6) are subject to the initial conditions $E_1(0) = E_{10}$, $E_2(0) = E_{20}$ and $\delta(0) = 1$; with $\beta(0) = \beta_0$ chosen to correspond to the physical frequency of the subharmonic, the specified \bar{U} and the initial physical length scale of the mean flow δ_0 . This length scale is identified with the initial half-

maximum slope thickness. The advection integrals are I_m , $I_1(\delta)$ and $I_2(\delta)$. Integrals involving wave disturbances are dependent on $\delta(x)$ through the dependence of the local instability properties on the local frequency parameter β , except for I_1 and I_2 that are very nearly constant and have been replaced in the equations by their average value. The production integrals are $I_{rs1}(\delta)$ and $I_{rs2}(\delta)$ and the mode-energy exchange integral is $I_{21}(\delta)$. The viscous dissipation integrals are I_d , $I_{d1}(\delta)$ and $I_{d2}(\delta)$. The Reynolds number is $Re = \bar{U}\delta_0/\nu$. The subscripts 1 and 2, as interpreted previously, denote the subharmonic and fundamental, respectively. The detailed definitions of these integrals are given in Appendix 1. Their physical meaning is identifiable through (3.1) - (3.3). The mean flow integrals I_m and I_d are constants for a fixed velocity-ratio parameter R , whereas integrals involving the wavy disturbances are tabulated functions of the dependent variable $\delta(x)$ again for a fixed R . It was sufficient to use the Rayleigh equation in obtaining the characteristics of such integrals (see, for instance, Liu and Merkin 1976), they are thus not explicit functions of the Reynolds number.

(c) Mode-dependent interaction integrals

Prior to discussing the numerical applications, it would be most instructive to show the behavior of the mode-related integrals in (3.4) - (3.6). These are "universal" functions of the local shear layer thickness $\delta(x)$, or more precisely of the local frequency parameter $\beta = 2\pi f\delta(x)/\bar{U}$ for a fixed frequency f . The value of the velocity ratio parameter R is taken to be

0.31. The mode viscous dissipation integral I_{dn} is shown in Figure 5 as function of β . The mode advection integral I_n slowly varies between 0.965 and 1 in the same interval of β and is thus not shown. The mode-production integral I_{rsn} is shown in Figure 3. The integrals I_{rs1} and I_{rs2} are the subharmonic and fundamental "production" integrals, respectively. Their sign controls the energy flow to or from the mean flow. When they are positive the disturbance wave component is amplified by extracting energy from the mean flow and when negative the disturbance is "damped" by returning energy to the mean motion. The latter phenomenon is rather similar to hydrodynamic stability interpretations and is now widely observed in developing free shear flows. The interpretation of $n = 1$ and 2 is that the frequency ratio $\beta_1 : \beta_2$ be maintained as 1: 2. That is, if the physical frequency of the fundamental (β_2) has the value $f_2 = 2f$ then the subharmonic component (β_1) has the value $f_1 = f$, both at the same $\delta(x)$. Thus, in Figure 3, if the fundamental mode is initiated at $\beta_2 \approx 0.4426$ where I_{rs2} is maximum, the subharmonic would be at $\beta_1 \approx 0.2213$ where I_{rs1} is smaller and to the left of the hump of the production-integral curve. In this case, as $\delta(x)$ increases the respective production integrals then traverse along this curve with I_{rs2} becoming negative first while I_{rs1} passes through its maximum value.

The binary mode-interaction integral I_{21} is shown in Figure 4, with the relative phase angle θ as a parameter. We have chosen to interpret I_{21} as a function of β_1 in Figure 4 (while keeping track of β_2 , for the same $\delta(x)$). The integral I_{21} ,

which represents the interaction between the fundamental and the subharmonic, controls the energy flow between the two modes via its magnitude and sign. The subharmonic draws energy from the fundamental when $I_{21} < 0$ and loses energy to the fundamental when $I_{21} > 0$. In turn the sign of this integral is controlled by the phase angle between the two modes θ and is of great significance to the role of the binary mode-interaction mechanism. In effect θ is the governing parameter that dictates whether the subharmonic grows at higher (Kelly 1967) or lower amplification rates than those dictated by linear stability analysis.

The present formulation is intended to solve the streamwise development problem from the use of the local linear theory in the evaluation of the interaction integrals. It is, however, crucial to reconcile any similarities with the pioneering work of Kelly (1967) for a parallel flow and weak nonlinearities. In the context of the present spatial problem, Kelly's analysis falls in the local region where the fundamental component is most amplified. The most amplified mode occurs at $\beta_2 = 0.4426$ in Figure 2 and thus $\beta_1 = 0.2213$, where the subharmonic is amplifying due to the mean flow. In Figure 4, where the horizontal axis is β_1 , a vertical line drawn from $\beta_1 = 0.2213$ cuts across values of the binary mode-interaction integral for various relative phase angle θ . For this situation, $0^\circ \leq \theta < 60^\circ$ give rise to $I_{21} < 0$, implying energy transfer from the fundamental to the subharmonic. Thus the mean flow amplification of the subharmonic component is augmented by the fundamental within this range of phase angles. The opposite is

true as $\theta \rightarrow \pi$ as shown in Figure 4 for $\beta_1 \approx 0.2213$. This is consistent with Kelly (1967). We again emphasize that the temporal, parallel flow problem that Kelly discussed occurs "momentarily" at one streamwise location corresponding to $\beta_2 \approx 0.4426$ and $\beta_1 \approx 0.2213$ in the context of the present developing shear layer problem. In our problem, the development of the amplitudes is a strong function of the initial and spectral conditions, dictated by the nonlinear interactions according to (3.4) - (3.6). The realistic outcome is not necessarily anticipated from considerations based on parallel flow.

4. RESULTS AND DISCUSSION

The theoretical formulation, presented in the previous sections of this paper, indicates that the initial conditions $(\beta_0, E_{20}, E_{10})$ along with the phase angle θ are parameters that play a very significant role in the development of the two interacting wave modes and, subsequently, the development of the shear layer. The phase angle, θ , between the fundamental wave component and its subharmonic, has been shown to be the sole parameter responsible for the nature of the interaction between these two wave-modes. The initial dimensionless frequency β_0 has two significant effects. It defines, on one hand, the initial amplification rate and the downstream amplification "history" of each wave from the interaction with the mean flow and on the other, the nature of the initial interaction between the two waves. The strength of the interaction between the waves as well

as that between the waves and the mean flow is also controlled by the initial energy densities E_{20} and E_{10} of the fundamental and subharmonic, respectively, as pointed out by Kelly (1967). Finally the Reynolds number Re_0 influences the intensity of viscous dissipation for all the components of the flow. This parameter is of minor importance in this formulation where the local linear solution is independent of the Reynolds number, and viscous dissipation is weak compared to the other mechanisms present.

We have solved the nonlinear interaction problem, formulated by equations (3.4) - (3.6), for different values of the controlling parameters, in order to bring forth their effect on the development of the shear layer and the interactions between the three components of the flow. These results are presented first. We then present results for conditions based on the experiment of Ho & Huang (1982) for purposes of comparing our theoretical results with their measurements.

(a) Effect of the phase angle θ

To better illustrate the role of the phase angle θ on the development of the shear layer and the energy content of the interacting modes, we have chosen to examine two cases. For fixed initial energy densities $E_{20} = 0.68 \cdot 10^{-4}$ and $E_{10} = 0.12 \cdot 10^{-4}$ and fixed Reynolds number $Re_0 = 71$ we have solved the interaction problem for low and high initial frequency parameters. We have carried out the calculations for various representative values of the phase angle. The initial frequency parameter characterizing each case is, by our choice, that of the

subharmonic wave.

(i) Low initial frequency parameter

The streamwise development of the energy levels of the fundamental (E_2) and subharmonic (E_1) waves, scaled by the corresponding initial values, are presented in Figure 6a for phase angles of 0° and 180° , as well as for the case where the direct wave interaction mechanism is artificially neglected. In the latter case, indirect coupling between the waves is through their nonlinear interactions with the mean flow. The initial subharmonic frequency parameter is taken to be $\beta_0 = 0.075$, giving a fundamental frequency of $2\beta_0 = 0.15$. The two modes start at a frequency parameter much smaller than the most amplified case in terms of linear stability theory (Figure 2). Naturally the fundamental experiences maximum amplification first while the subharmonic grows at a lower rate as it can be seen from Figure 6a.

In the early stage of the development of the two modes when $\theta = 0^\circ$ the subharmonic draws energy from the fundamental component because the two-mode interaction integral I_{21} is negative. Therefore the subharmonic is growing, in that region, at higher amplification rates than those predicted by linear stability analysis from its interaction with the mean flow only. This is evident from the comparison with the decoupled case in the region $0 < x/\delta_0 < 55$, as presented in Figure 6a. This situation persists until the fundamental goes through maximum amplification (for $\beta_2 \leq 0.6$ as indicated in the discussion of the two-mode interaction integral) and is in agreement with the

conclusion of Kelly (1967). In the same region, for the case of $\theta = 180^\circ$, the interaction integral I_{21} is positive and the subharmonic loses energy to the fundamental component, thus growing at a lower amplification rate, as shown in Figure 6a. The comparison with the decoupled case, in this region, shows that the wave interaction has a greater effect on the development of the subharmonic because its interaction with the mean flow is much weaker than that of the fundamental. The extraction of energy from the mean flow is the dominant energy supply for the fundamental component and is responsible for the peak in E_2 . In the strongly nonlinear region, for values of the fundamental frequency parameter β_2 higher than 0.6 ($x/\delta_0 > 55$ in Figure 6a) the sign of the two-mode interaction term, $I_{21} E_1 E_2^{1/2} / \delta^{3/2}$, in equations (3.5) and (3.6) is reversed and therefore the subharmonic loses energy to the fundamental component when $\theta = 0^\circ$. Because of this interaction the subharmonic wave grows at a lower rate and the fundamental persists downstream even when it starts losing energy to the mean flow. This mechanism accounts for the lower and later peak of the subharmonic energy E_1 compared to the decoupled case.

In the case of $\theta = 180^\circ$, the opposite situation to the $\theta = 0^\circ$ case takes place in the strongly nonlinear region. The subharmonic drawing energy from the fundamental grows faster and to a higher peak, while the fundamental is quickly damped by the combined loss of energy to the subharmonic component and mean flow. The wave interaction is the decisive factor for the survival of the fundamental far downstream, since there it is

being damped by returning energy to the mean flow, where $I_{rs2} < 0$ (Figure 3). The subharmonic is affected by the wave interaction to a relatively small extent. This becomes obvious from the comparison with the decoupled case in Figure 6a.

From (3.4), it is obvious that the mean flow will spread as long as energy is lost from the mean flow, whether it is due to viscous dissipation or energy transfer to the fluctuations. The resulting growth of the mean flow is shown in Figure 6b. The initial rapid growth is governed by the strong interaction of the amplified fundamental disturbance with the mean flow and remains unaffected by the interaction between the two disturbances which in this region is very weak. The first plateau is due to the peak in the fundamental, the second due to the peaking of the subharmonic. These plateaus are associated with the observed phenomenon of negative energy production from the mean (see, for instance, Fiedler, Dziomba, Mensing & Rosgen 1981) that occurs when the sign of the Reynolds stress $-\overline{uw}$ of a particular wave mode of coherent structure is opposite to that of the mean flow rate of strain $\frac{\partial U}{\partial z}$. and the production integral $I_{rsn} < 0$, thus tending to halt the shear layer growth. After the first plateau the growth of the mean flow is again rapid because of the amplification of the subharmonic from extraction of energy from the mean flow. However, the interaction of the two modes seems to play some role on this development. In the case of $\theta = 180^\circ$ the growth of the mean is somewhat steeper because of the extra energy that is channeled into the subharmonic wave from the fundamental component. The opposite is true in the case

where $\theta = 0^\circ$ and the plateau that results from the saturation of the subharmonic is somewhat lower. The shear layer thickness due to the subharmonic is very nearly double that due to the fundamental in Figure 6b. That is, the ratio of the two plateau is nearly two. However, this is somewhat dependent upon the initial conditions, as we will show later, and ought not to be a general rule.

(ii) High initial frequency parameter

The streamwise development of the energy levels of the fundamental (E_2) and subharmonic (E_1) waves, scaled by the corresponding initial values, are presented in Figure 7a for phase angles of 0° , 80° and 180° , as well as for the decoupled case. The initial energy densities and Reynolds number are the same as in the case of low initial frequency parameter while the value of the latter is taken to be $\beta_0 = 0.18$ for the subharmonic and $2\beta_0 = 0.36$ for the fundamental component. The latter is slightly less than the initially most amplified Strouhal frequency.

Both disturbances experience a higher initial amplification than in the previous case because their initial frequency parameters are closer to the one corresponding to the most amplified disturbance. A consequence of this fact is that the two-wave interaction mechanism is much weaker than the interaction of both wave components with the mean. Subsequently the initial development of E_1 and E_2 is essentially unaffected by the modal interaction as shown in Figure 7a. The two-wave interaction becomes important in the strongly nonlinear region,

after the fundamental has reached its peak, in the same manner as in the previous case of low initial frequency parameter. The case of $\theta = 80^\circ$ is characterized by a weaker modal interaction than that of $\theta = 0^\circ$, as one can expect from the magnitude of the respective interaction integrals (Figure 4). The energy flow is from the subharmonic to the fundamental component for both of these phase angles, in the strongly nonlinear region. The resulting growth of the mean flow, which is shown in Figure 7b, indicates the same general trends observed for the low initial frequency parameter case.

The two-wave interaction mechanism has a dual effect on the modal development. It affects the amplification rate of the subharmonic directly by providing energy from the fundamental and indirectly by increasing the energy gained from the mean, since this gain is proportional to E_1 . These two effects are of course coupled. The direct two-wave interaction mechanism is represented by the term, $I_{21}E_1E_2^{1/2}/\delta^{3/2}$, and is shown in Figure 7c. The indirect wave-interaction effect can be realized by comparing the mean-subharmonic interaction term, $I_{rs1}E_1/\delta$, for the cases of $\theta = 0^\circ$ and $\theta = 180^\circ$ as presented in Figure 7d. It also appears from the observation of Figures 7c and 7d that the indirect effect of the two-wave interaction mechanism is more significant, because the energy exchange with the mean is the controlling factor in the growth of the subharmonic in this particular case.

(b) Effect of the initial frequency parameter β_0 .

The streamwise development of the energy levels of the two

wave-modes are shown in Figure 8a for three different initial frequency parameters and for a phase angle $\theta = 0^\circ$. The initial frequency parameter, as pointed out earlier, defines the initial amplification rate of the disturbances from their interaction with the mean flow; it also controls the overall amount of energy that each individual disturbance will extract from the mean flow throughout its development. In the case of $\beta_0 = 0.30$ the disturbance characterized by $2\beta_0 = 0.6$ starts out at an amplification rate lower than that of its subharmonic and past its maximum amplification rate as it can be seen from the mean flow interaction integral in Figure 3. Subsequently the wave characterized by $\beta_0 = 0.3$ dominates throughout the development of the flow, as shown in Figure 8a and is actually the fundamental disturbance. The wave characterized by $2\beta_0$ is its first harmonic and despite the fact that the two-wave interaction mechanism acts in its favour ($\theta = 0^\circ$), its role in the development of the flow is negligible. This is also apparent from the development of the mean flow for this case shown in Figure 8b, where the single plateau is attributed to the saturation of E_1 only.

In general decrease of the initial frequency parameter will increase the downstream amplification "history" of each wave. The peaks in E_1 and E_2 are higher and occur at a later stage as the initial frequency parameter is decreased, because of the implied increase of the overall energy extracted from the mean. The growth of the mean flow is more pronounced for lower values of the initial frequency parameter due to the same physical effect (Figure 8b).

The discussion so far has been limited to the "direct" effect of the initial frequency parameter on the development of the modal energy densities which is a consequence of the interaction with the mean flow. The effect of β_0 on the modal interaction mechanism is apparent from the comparison between the results presented in Figures 6a and 7a for low and high β_0 respectively and for the case, say, where $\theta = 0^\circ$. For high β_0 , as pointed out earlier, the early and favourable to the subharmonic disturbance interaction is practically absent unlike the case where the initial frequency parameter is low. This effect of β_0 on the modal interaction mechanism is, however, negligible compared to that of the phase angle. According to the above observations, we can conclude that the effect of the initial frequency parameter is essentially confined to the one influencing the interaction between the waves and the mean flow.

(c) Effect of the initial energy density of the subharmonic.

The results of our calculations for three different initial energy densities of the subharmonic are given in Figures 9a, 9b, 9c and 9d with all other initial parameters being fixed and a phase angle $\theta = 0^\circ$. The peaks in E_1/E_{10} are proportional to E_{10} ; therefore, the subharmonic reaches the same approximately peak level irrespectively of its initial density. The interaction of the subharmonic with the mean becomes maximum earlier with increasing E_{10} as can be seen from Figure 9c, where we show the development of the wave-mean interaction term. This accounts for the earlier peaking of E_1 and the subsequent earlier

second plateau of the mean flow development shown in Figure 9b. The level of this plateau is independent of the initial density of the subharmonic as is the peak level of E_1 . The two-wave interaction term, presented in Figure 9d, becomes strong earlier with increasing E_{10} . For this case of $\theta = 0^\circ$ the two-wave interaction in the early stages of the modal development is in favor of the subharmonic, as discussed in an earlier section. These two observations explain the weakening of the interaction of the fundamental with the mean and the lower peak of E_2 with increasing E_{10} . This is also in agreement with Kelly's mechanism and results in a less prominent first plateau in the growth of the mean as we increase the initial subharmonic density.

(d) Effect of the initial energy density of the fundamental.

The results of our calculations for three different initial energy densities of the fundamental are shown in Figures 10a, 10b, 10c and 10d. The peak value of the fundamental energy level, E_2 , is shown to be independent of its initial energy density since E_2/E_{20} is proportional to E_{20} in Figure 10a. The peak value of the subharmonic also remains unaffected. Therefore the plateau levels in the growth of the mean presented in Figure 10b are independent of E_{20} . The increase of the initial energy density of the fundamental intensifies the interaction with the mean (Figure 10c) in its amplification region and therefore causes a faster growth of the shear-layer as shown in Figure 10b. The interaction term between the subharmonic and the mean

flow and the two-mode interaction term are inversely proportional to δ and $\delta^{3/2}$ (see equations (3.5) and (3.6)). Therefore, the faster growth of the mean accounts for the shift in the peaks of these two terms downstream (Figures 10c and 10d), the subsequent weakening of the subharmonic and faster growth of the mean after the first plateau.

(e) Effect of the initial Reynolds Number

The development of the energy levels of the fundamental and subharmonic disturbances, scaled by the corresponding initial values, are given in Figure 11a for $Re_0 = 35.5$ and 71. It can be seen that viscous dissipation has a very weak effect on the development of the modes. The fundamental and subharmonic peaks occur earlier and at a higher level with increasing Re_0 . This of course was expected since viscous effects are weaker with increasing Reynolds number. The development of the mean flow is shown in Figure 11b. The growth of the mean flow is faster for high Re_0 in the initial stages before the first plateau and is related to the growth of the fundamental. One would expect a slower growth of the mean when the Reynolds number is high, because of the viscous term $(\frac{1}{Re_0} Id/\delta)$ in equation (3.4). However, this term is negligible compared to the wave production terms; thus the development of the mean is controlled primarily by the interaction with the two disturbances. We should point out at this point that the use of the inviscid local solutions for the disturbances renders the Interaction integrals independent of the Reynolds number; hence viscous effects have

not been accounted for in full.

(f) Comparisons with experimental results of

Ho and Huang (1982)

The results of our calculation presented in this section are based on the experimental conditions corresponding to the measurements performed by Ho and Huang (1982). The initial subharmonic frequency parameter is taken to be $\beta_0 = 0.26$, giving a fundamental $2\beta_0 = 0.52$ which is very nearly at the maximum amplification rate according to the linear theory. These values were based on the initial maximum slope thickness δ_0 at a location 1.43 cm downstream of the splitter plate, where the initial wake type profile has developed into a hyperbolic tangent shear layer profile, as reported by Ho and Huang (1982). The origin in the calculation, $x = 0$, is taken to be at the experimental 1.43 cm location. The relative phase between the fundamental and the subharmonic is left arbitrary (and therefore unknown) in the experiment. We carried out the calculations for three different phase angles, namely $\theta = 0^\circ$, 80° and 180° .

The streamwise development of the energy levels of the streamwise component of the fundamental (Eu_2) and subharmonic (Eu_1) is qualitatively in very good agreement with the experiment as one can see from Figure 12a, particularly for the $\theta = 80^\circ$ case. The location of the peaks in Eu_1 and Eu_2 are well in agreement with the experiment although the peak values themselves are underestimated. The growth of the shear layer shown in Figure 12b also compares well with the experiments (Ho & Huang

1982) both qualitatively and quantitatively, in the region where the two wave modes are developing. The plateaus (attributed to the energy flow from the mean to the disturbances according to our previous discussion) as well as the approximate doubling of the thickness are evident in both the experiment and our results. In Ho and Huang's (1982) experiments, the shear layer continues to spread after the plateau regions (Figure 12b); it is most likely that transition has taken place in that the existing fine-grained turbulence having been sufficiently strained by the coherent structures is now contributing towards the mean flow spreading rate via the fine-grained turbulence Reynolds stress mechanism. This mechanism is not present in our formulation since we have not taken under account the fine grained turbulence. Therefore this latter spread of the mean flow cannot be predicted by our calculations.

Apart from the fine grained turbulence, there are many other less dominant disturbance wave modes present in the experiments of Ho and Huang (1982) to which the shear layer is sensitive. This fact together with the arbitrariness of the phase angle in the experiment leads to the conclusion that the quantitative details of the shear layer are not expected to be described by the idealized two-mode problem in the absence of weak fine-grained turbulence and other (not necessarily weak) modes. However, the problem solved here brings out the dominant physical mechanisms in the growth and decay of the overlapping fundamental and subharmonic disturbances, as well as the important effect of the initial conditions and relative phase angle.

This work was partially supported by the National Aeronautics and Space Agency, Langley Research Center through Grant NAG1-379, Lewis Research Center through Grant NAG3-673; and the National Science Foundation, Fluid Mechanics and Hydraulics Program through Grant MSM83-20307.

APPENDIX 1. TWO MODE INTERACTION INTEGRALS

$$\begin{aligned} \text{Im} = & -\frac{1}{2} \left[\int_{-\infty}^0 (1-R \tanh \eta) [(1-R \tanh \eta)^2 - (1+R)^2] d\eta + \int_0^{\infty} (1-R \tanh \eta) [(1-R \tanh \eta)^2 - \right. \\ & \left. - (1-R)^2] d\eta \right] = 2R^2(3/2 - \ln 2) \end{aligned}$$

$$I_1(\delta) = 1 - R \int_{-\infty}^{+\infty} \tanh \eta \{ |\phi_1'|^2 + |a_1 \phi_1|^2 \} d\eta$$

$$I_2(\delta) = 1 - R \int_{-\infty}^{+\infty} \tanh \eta \{ |\phi_2'|^2 + |a_2 \phi_2|^2 \} d\eta$$

$$I_{rs1} = 2R \int_{-\infty}^{+\infty} \text{sech}^2 \eta \text{Im}(a_1 \phi_1 \bar{\phi}_1') d\eta$$

$$I_{rs2} = 2R \int_{-\infty}^{+\infty} \text{sech}^2 \eta \text{Im}(a_2 \phi_2 \bar{\phi}_2') d\eta$$

$$I_{21} = 2 \int_{-\infty}^{+\infty} \text{Im} \{ e^{i\theta} \{ \bar{a}_2 \{ \bar{\phi}_2' (\phi_1'^2 + a_1^2 \phi_1) + a_1 \bar{a}_2 \bar{\phi}_2 \phi_1 \phi_1' \} + a_1 \phi_1 \phi_1' \bar{\phi}_2'' \} \} d\eta$$

$$I_d = \int_{-\infty}^{+\infty} R^2 \text{sech}^4 \eta d\eta = \frac{4R^2}{3}$$

$$I_{d1} = 2|a_1|^2 + 2 \int_{-\infty}^{+\infty} \{ |\phi_1''|^2 + |a_1 \phi_1'|^2 \} d\eta$$

$$I_{d2} = 2|a_2|^2 + 2 \int_{-\infty}^{+\infty} \{ |\phi_2''|^2 + |a_2 \phi_2'|^2 \} d\eta$$

where Im denotes the imaginary part and $\bar{\phi}$ denotes the complex conjugate of ϕ .

REFERENCES

- Browand, F. K. 1966. An Experimental Investigation of the Instability of an Incompressible Separated Shear Layer. J. Fluid Mech. 26,281-307.
- Fiedler, H. E., Dziomba, B., Mensing, P. & Rösgen, T. 1981. Initiation, Evolution and Global Consequences of Coherent Structures in Turbulent Shear Flows. In The Role of Coherent Structures in Modelling Turbulence and Mixing, Lecture Notes in Physics, ed. J. Jimenez, 136,219-51. Berlin/Heidelberg/New York:Springer.
- Freymuth, P. 1966. On Transition in a Separated Laminar Boundary Layer. J. Fluid Mech. 25,683-704.
- Ho, C. M. & Huang, L. S. 1982. Subharmonics and Vortex Merging in Mixing Layers. J. Fluid Mech. 119,443-73.
- Kelly, R. E. 1967. On the Stability of an Inviscid Shear Layer Which is Periodic in Space and Time. J. Fluid Mech. 27,657-89.
- Lin, C. C. 1955. The Theory of Hydrodynamic Stability. Cambridge Univ. Press.
- Liu, J. T. C. 1981. Interaction Between Large-Scale Coherent Structures and Fine-Grained Turbulence in Free Shear Flows. In Transition and Turbulence, pp. 167-214. New York/London:Academic.
- Liu, J. T. C. & Nikitopoulos, D.. 1982. Mode Interactions in Developing Shear Flows. Bull. Am. Phys. Soc 27, 1192.
- Mack, L. M. 1965. Computation of the Stability of the Laminar Compressible Boundary Layer. Meth. in Comp. Physics, V. 4, pp. 274-299.
- Miksad, R. W. 1972. Experiments on the Nonlinear Stages of Free Shear Layer Transition. J. Fluid Mech. 56,695-719.
- Miksad, R. W. 1973. Experiments on Nonlinear Interactions in the Transition of a Free Shear Layer. J. Fluid Mech. 59,1-21.
- Nikitopoulos, D. E. 1982. Nonlinear Interaction Between Two Instability Waves in a Developing Shear Layer. MS thesis. Brown Univ., Providence, R.I.
- Wille, R. 1963. Beiträge zur Phänomenologie der Freistrahlen. Z. Flugwiss. 11,222-33.
- Williams, D. R., Hama, F. R. 1980. Streaklines in a Shear Layer Perturbed by Two Waves. Phys. Fluids 23,442-47.
- Winant, C. D., Browand, F. K. 1974. Vortex Pairing, the Mechanism of Turbulent Mixing-Layer Growth at Moderate Reynolds Number. J. Fluid Mech. 63,237-55.
- Wynanski, I., Fiedler, H. E. 1970. The Two-Dimensional Mixing Region. J. Fluid Mech. 41,327-361.

Zaat, J. A. 1958. In "Boundary Layer Research," (H. Görtler ed.), p. 127.
Berlin:Springer.

FIGURE CAPTIONS

- Figure 1 The mixing layer schematic.
- Figure 2 Amplification rates $-\alpha_1$ versus frequency parameter β .
- Figure 3 Mode-production integral I_{rsn} as function of frequency parameter β .
- Figure 4 a,b Binary mode-interaction integral I_{21} as function of frequency parameter β with relative phase angle θ as a parameter.
- Figure 5 Mode viscous dissipation integral I_{dn} as function of frequency parameter β .
- Figure 6a Development of modal energy content for low initial frequency
 parameter ($\theta = 0^\circ, 180^\circ$ and decoupled case; $E_{10} = 0.12 \times 10^{-4}$,
 $E_{20} = 0.68 \times 10^{-4}$, $\beta_0 = 0.075$, $Re_0 = 71$).
- Figure 6b Mean flow growth for low initial frequency parameter ($\theta=0^\circ, 180^\circ$
 and decoupled case; $E_{10} = 0.12 \times 10^{-4}$, $E_{20} = 0.68 \times 10^{-4}$,
 $\beta_0 = 0.075$, $Re_0 = 71$).
- Figure 7a Development of modal energy content for high initial frequency
 parameter ($\theta=0^\circ, 80^\circ, 180^\circ$ and decoupled case; $E_{10} =$
 0.12×10^{-4} , $E_{20} = 0.68 \times 10^{-4}$, $\beta_0 = 0.18$, $Re_0 = 71$).

- Figure 7b Mean flow growth for high initial frequency parameter
 $(\theta=0^\circ, 80^\circ, 180^\circ \text{ and decoupled case; } E_{10} = 0.12 \times 10^{-4},$
 $E_{20} = 0.68 \times 10^{-4}, \beta_0 = 0.18, Re_0 = 71).$
- Figure 7c Mode-production term development for high initial frequency
parameter $(\theta = 0^\circ, 180^\circ; E_{10} = 0.12 \times 10^{-4}, E_{20} = 0.68 \times 10^{-4},$
 $\beta_0 = 0.18, Re_0 = 71).$
- Figure 7d Binary mode-interaction term development for high initial
frequency parameter $(\theta = 0^\circ, 180^\circ; E_{10} = 0.12 \times 10^{-4}, E_{20} = 0.68$
 $\times 10^{-4}, \beta_0 = 0.18, Re_0 = 71).$
- Figure 8a Development of modal energy content: effect of initial
frequency parameter $(\beta_0 = 0.075, 0.18, 0.3; E_{10} = 0.12 \times 10^{-4},$
 $E_{20} = 0.68 \times 10^{-4}, \theta = 0^\circ, Re_0 = 71).$
- Figure 8b Mean flow growth: effect of initial frequency parameter $(\beta_0 =$
 $0.075, 0.18, 0.3; E_{10} = 0.12 \times 10^{-4}, E_{20} = 0.68 \times 10^{-4},$
 $\theta = 0^\circ, Re_0 = 71).$
- Figure 9a Development of modal energy content: effect of initial
subharmonic energy density. $(E_{10} = 1.2, 0.4, 0.12 \times 10^{-4};$
 $E_{20} = 0.68 \times 10^{-4}, \beta_0 = 0.075, \theta = 0^\circ, Re_0 = 71).$

Figure 9b Mean flow growth: effect of initial subharmonic energy density ($E_{10} = 1.2, 0.4, 0.12 \times 10^{-4}$; $E_{20} = 0.68 \times 10^{-4}$, $\beta_0 = 0.075$, $\theta = 0^\circ$, $Re_0 = 71$).

Figure 9c Mode-production term development: effect of initial subharmonic energy density ($E_{10} = 1.2, 0.4, 0.12 \times 10^{-4}$; $E_{20} = 0.68 \times 10^{-4}$, $\beta_0 = 0.075$, $\theta = 0^\circ$, $Re_0 = 71$).

Figure 9d Binary mode-interaction term development: effect of subharmonic energy density ($E_{10} = 1.2, 0.4, 0.12 \times 10^{-4}$; $E_{20} = 0.68 \times 10^{-4}$, $\beta_0 = 0.075$, $\theta = 0^\circ$, $Re_0 = 71$).

Figure 10a Development of modal energy content: effect of initial fundamental energy density ($E_{20} = 13.6, 6.8, 0.6 \times 10^{-5}$; $E_{10} = 0.12 \times 10^{-4}$, $\beta_0 = 0.075$, $\theta = 0^\circ$, $Re_0 = 71$).

Figure 10b Mean flow growth: effect of initial fundamental energy density ($E_{20} = 13.6, 6.8, 0.6 \times 10^{-5}$; $E_{10} = 0.12 \times 10^{-4}$, $\beta_0 = 0.075$, $\theta = 0^\circ$; $Re_0 = 71$).

Figure 10c Mode-production term development: effect of initial fundamental energy density ($E_{20} = 13.6, 6.8, 0.6 \times 10^{-5}$; $E_{10} = 0.12 \times 10^{-4}$, $\beta_0 = 0.075$, $\theta = 0^\circ$, $Re_0 = 71$).

Figure 10d Binary mode-interaction term development: effect of initial fundamental energy density ($E_{20} = 13.6, 6.8, 0.6 \times 10^{-5}$; $E_{10} = 0.12 \times 10^{-4}$, $\beta_0 = 0.075$, $\theta = 0^\circ$, $Re_0 = 71$).

Figure 11a Development of modal energy content: effect of initial Reynolds No. ($Re = 71, 35.5$; $E_{10} = 0.12 \times 10^{-4}$, $E_{20} = 0.68 \times 10^{-4}$, $\beta_0 = 0.075$, $\theta = 0^\circ$).

Figure 11b Mean flow growth: effect of initial Reynolds No. ($Re = 71, 35.5$; $E_{10} = 0.12 \times 10^{-4}$, $E_{20} = 0.68 \times 10^{-4}$, $\beta_0 = 0.075$, $\theta = 0^\circ$).

Figure 12a Development of modal energy content: Comparison with Ho and Huang (1982) experiment. ($\theta = 0^\circ, 80^\circ$ and 180° ; $Eu_{10} = 0.16 \times 10^{-4}$, $Eu_{20} = 0.48 \times 10^{-3}$, $\beta_0 = 0.26$, $Re_0 = 81$).

Figure 12b Mean flow growth: Comparison with Ho and Huang (1982) experiment. ($\theta = 0^\circ, 80^\circ$ and 180° : $Eu_{10} = 0.16 \times 10^{-4}$, $Eu_{20} = 0.48 \times 10^{-3}$, $\beta_0 = 0.26$, $Re_0 = 81$).

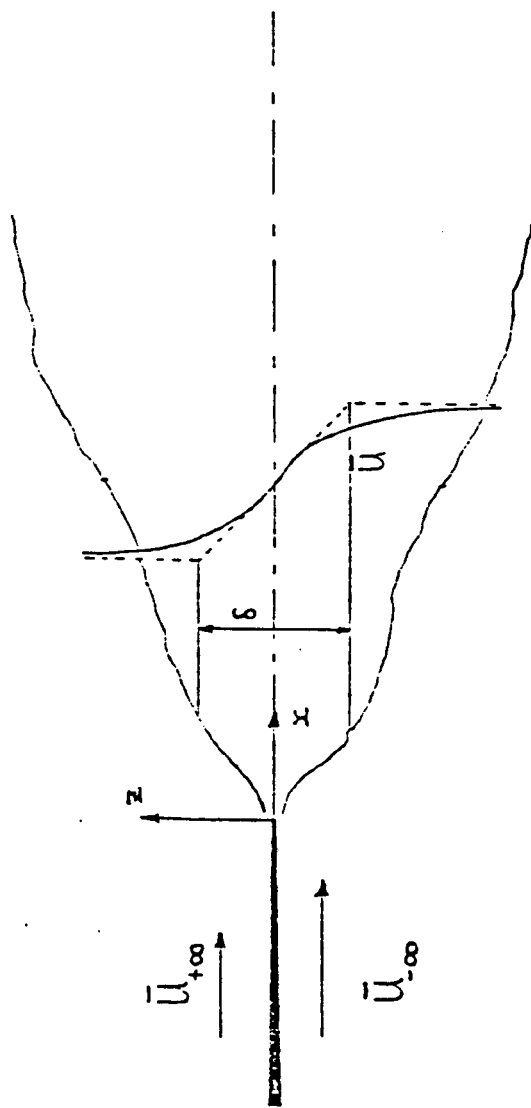


FIG-1

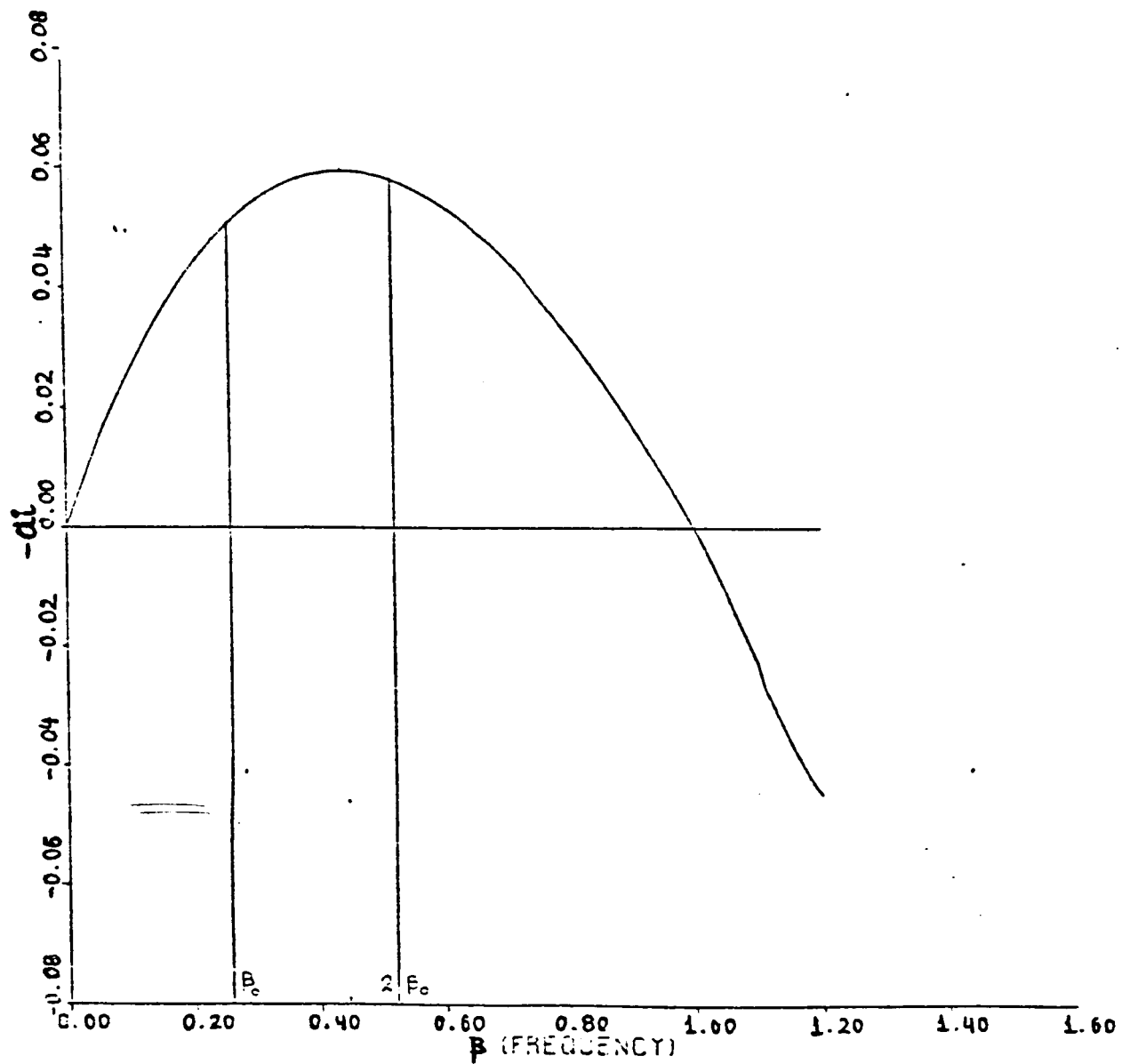


FIG 2

I_{rsn} vs. β

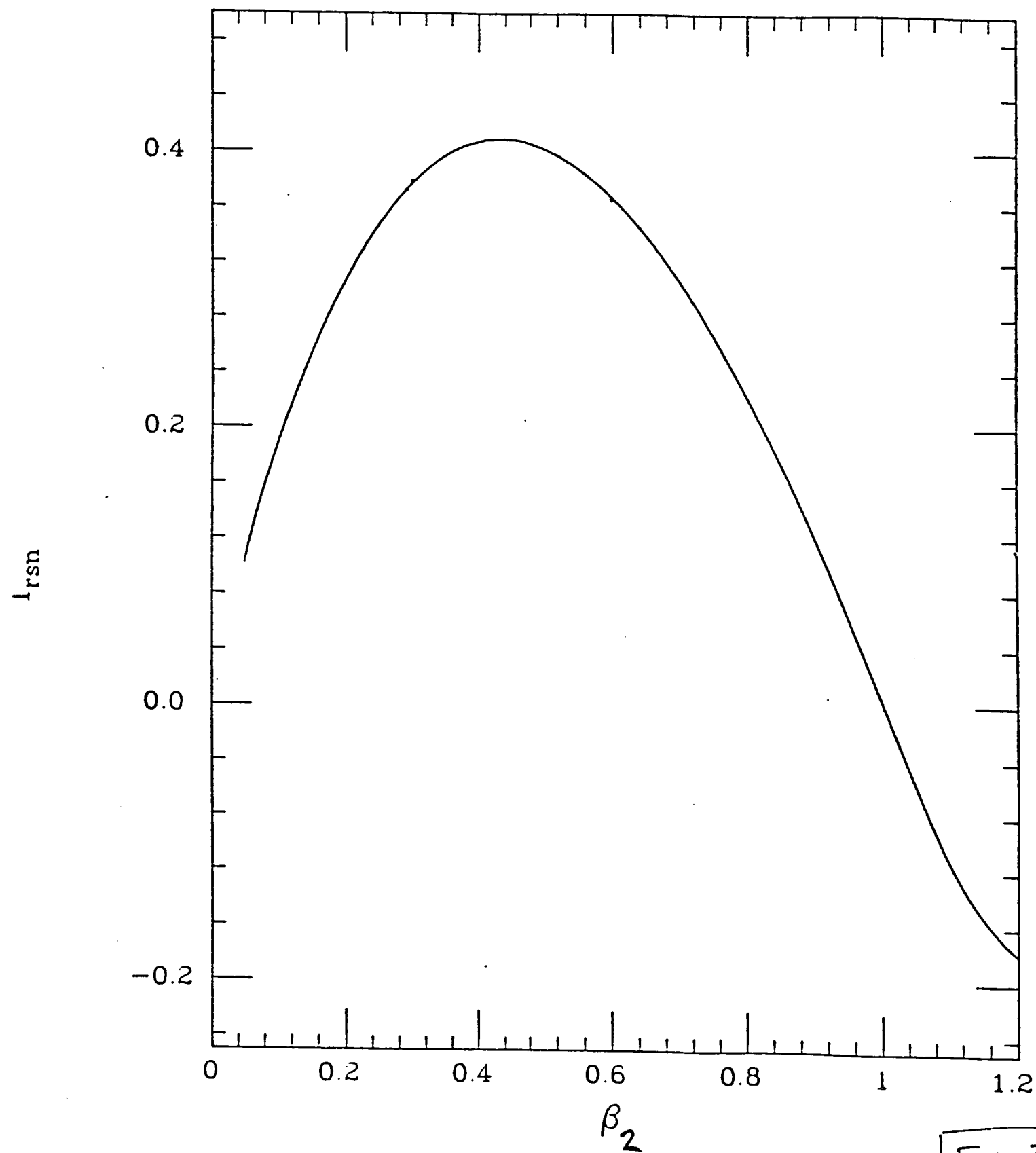


Fig 3.

I_{12}^1 vs. β

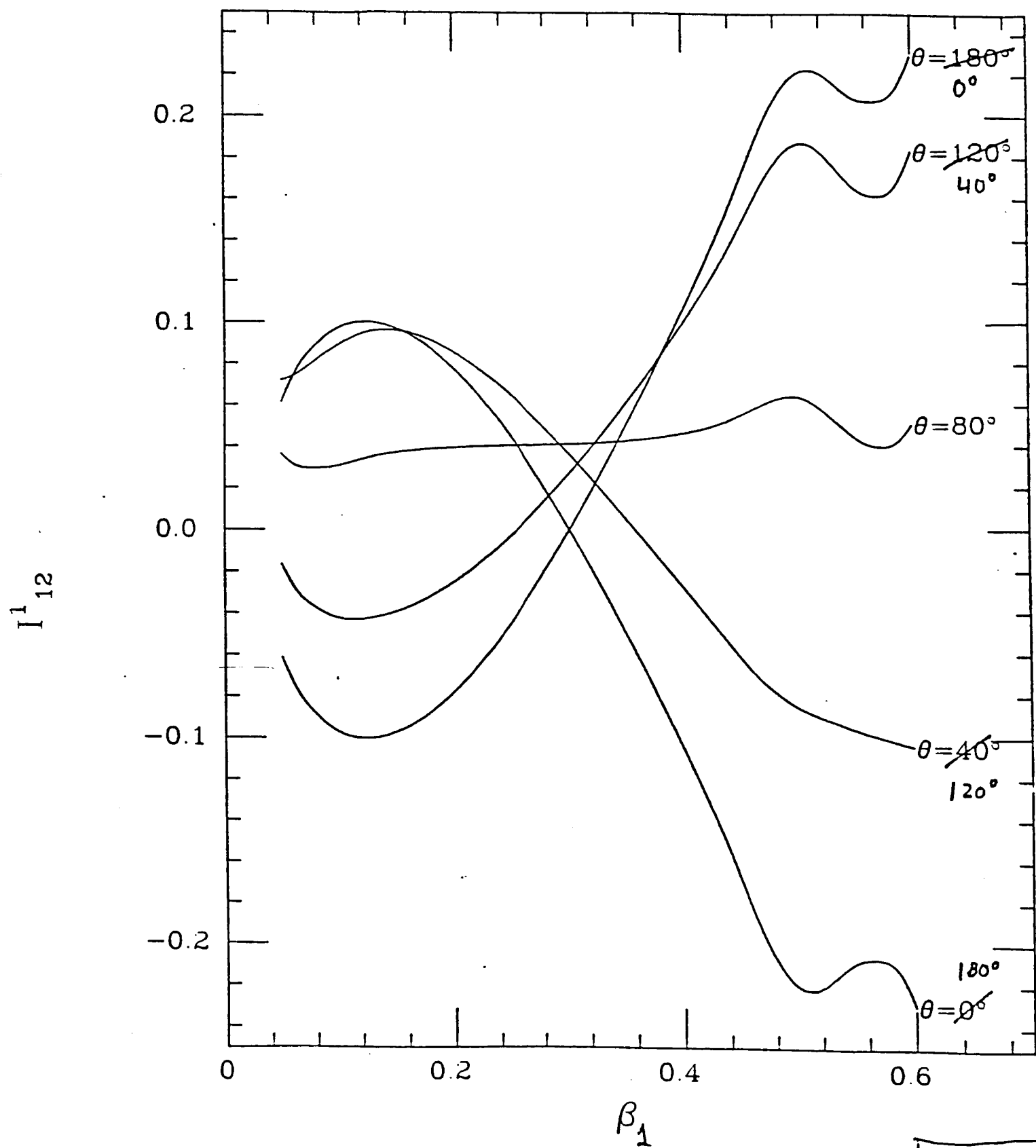


FIG 4a

I_{12}^1 vs. β

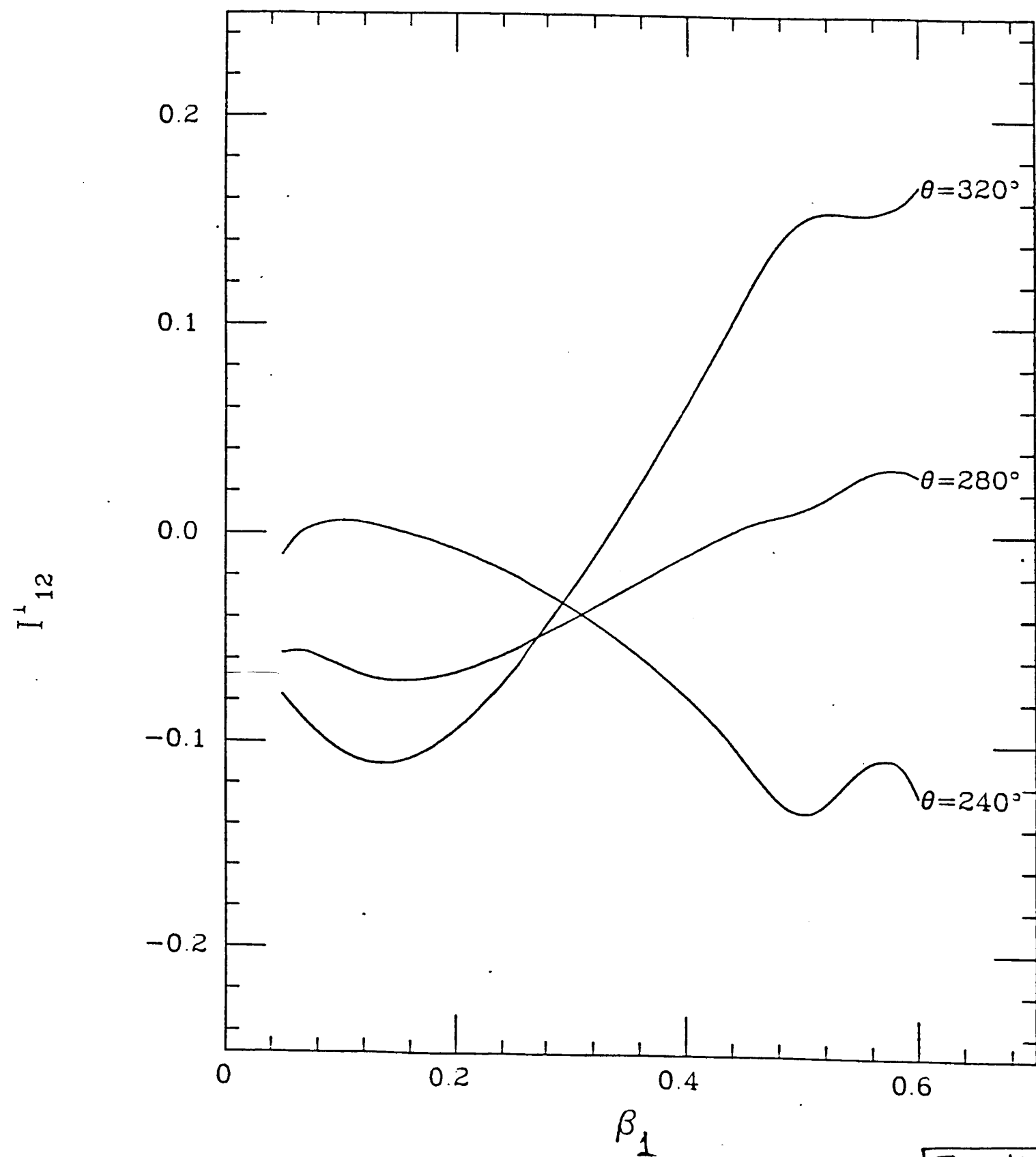


FIG 4b.

I_{dn} VS. β

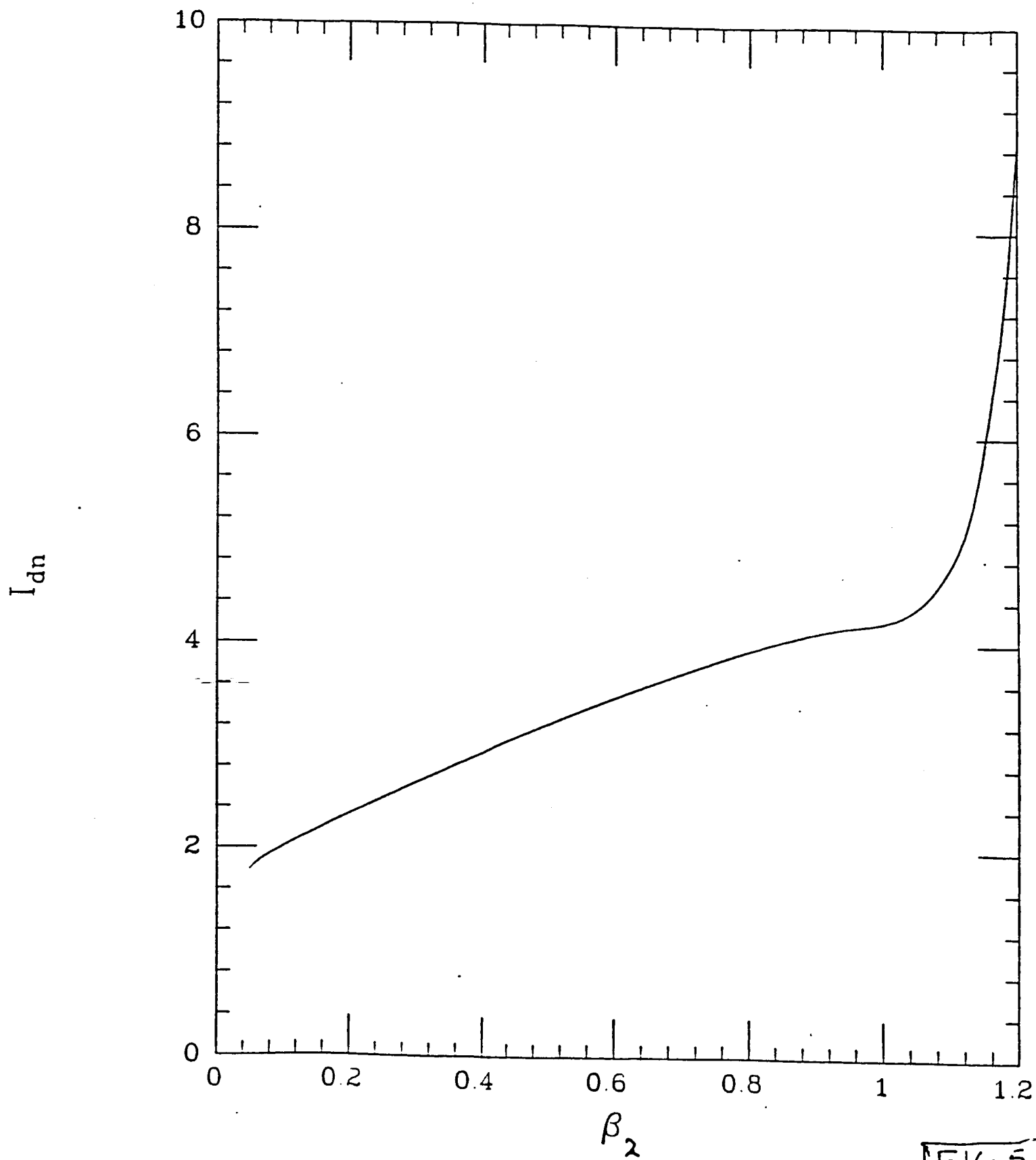


FIG 5

$E_1(0) = .12 \cdot 10^{-4}, E_2(0) = .68 \cdot 10^{-4}, Re_0 = 71, \beta_0 = .075$

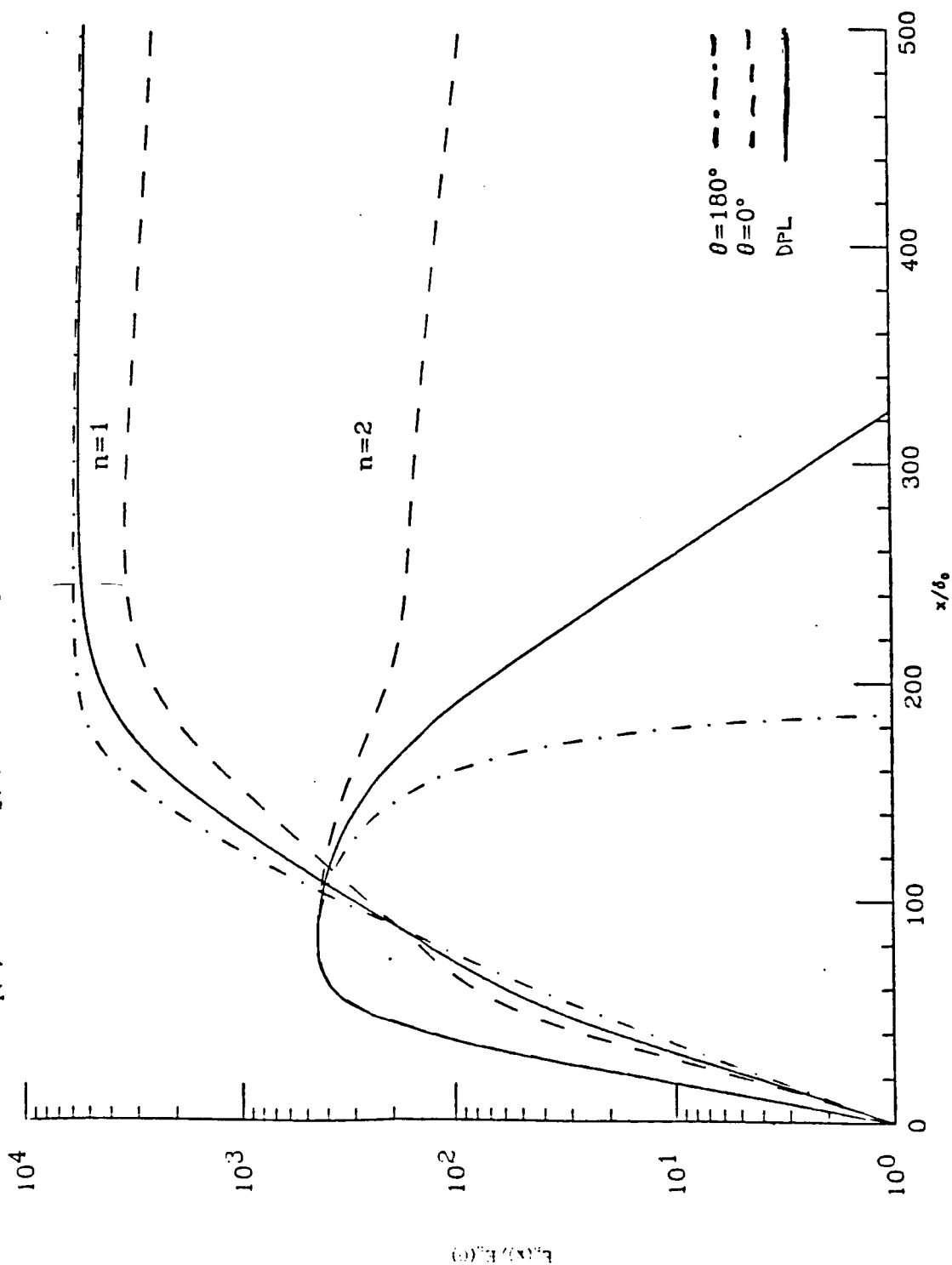


FIG 6a

$$E_1(0) = .12 \quad 10^{-4}, E_2(0) = .68 \quad 10^{-4}, Re_0 = 71, \beta_0 = .075$$

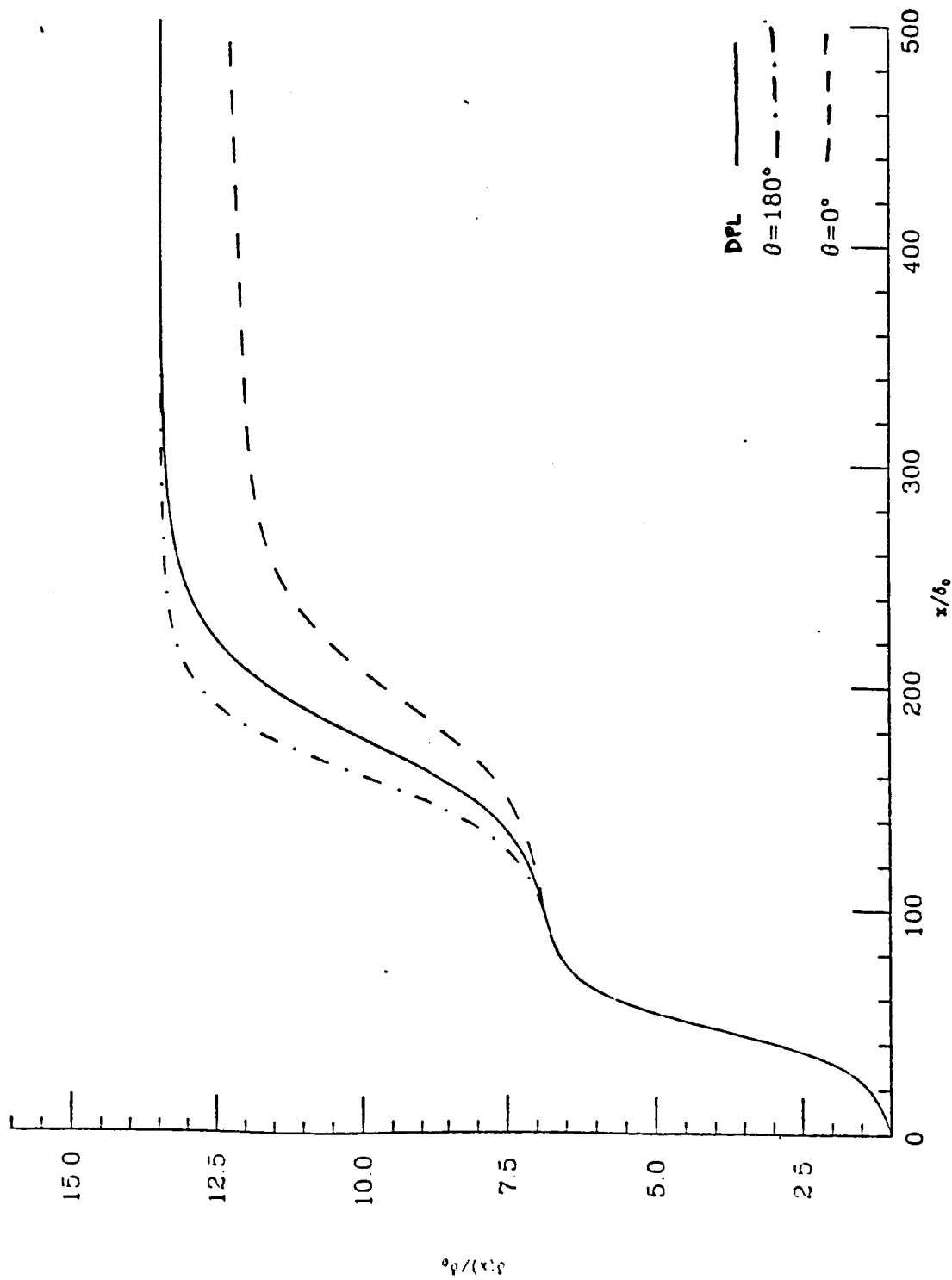


FIG 6b

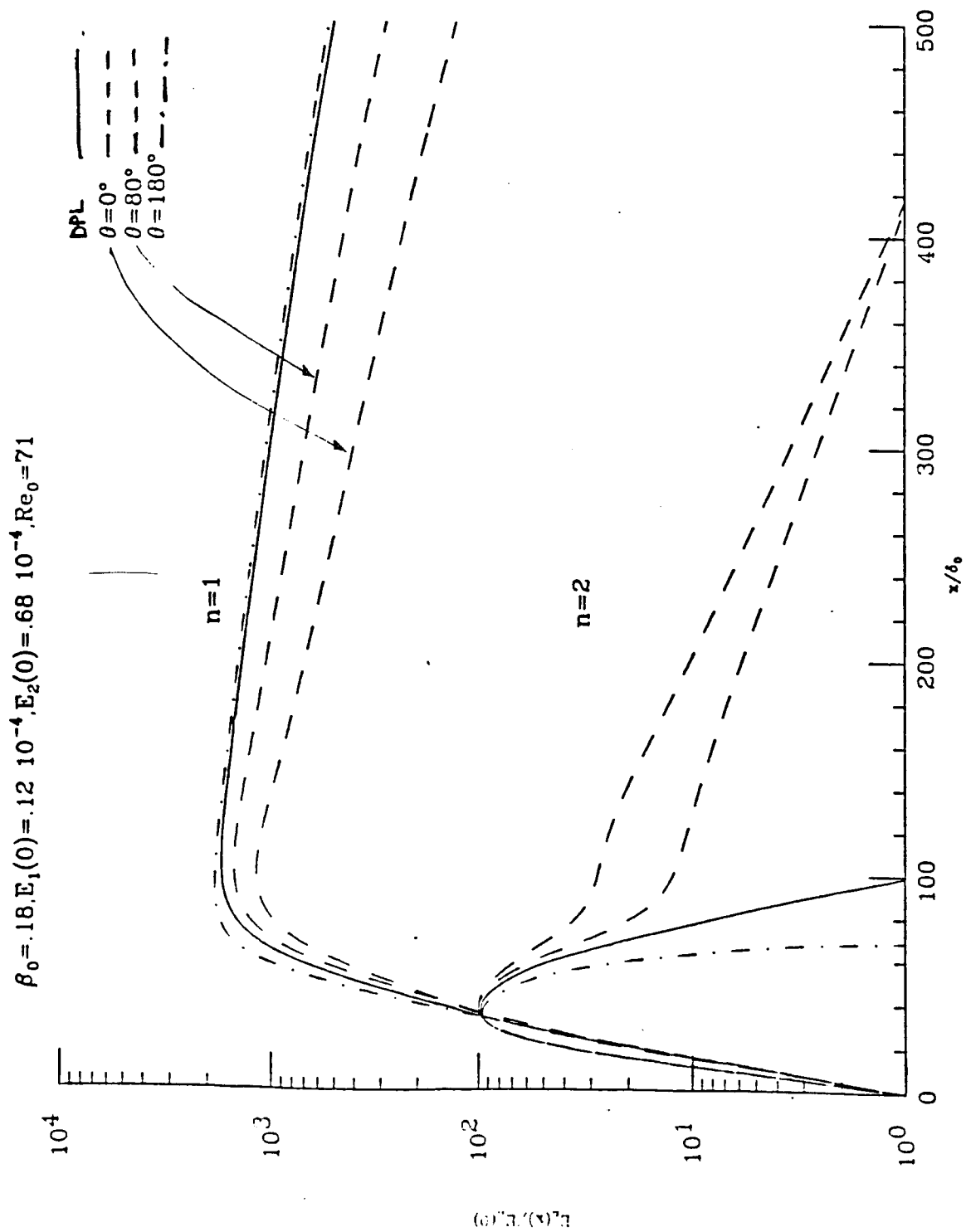


FIG 7a

$\beta_0 = .18, E_1(0) = .12 \cdot 10^{-4}, E_2(0) = .68 \cdot 10^{-4}, Re_0 = 71$

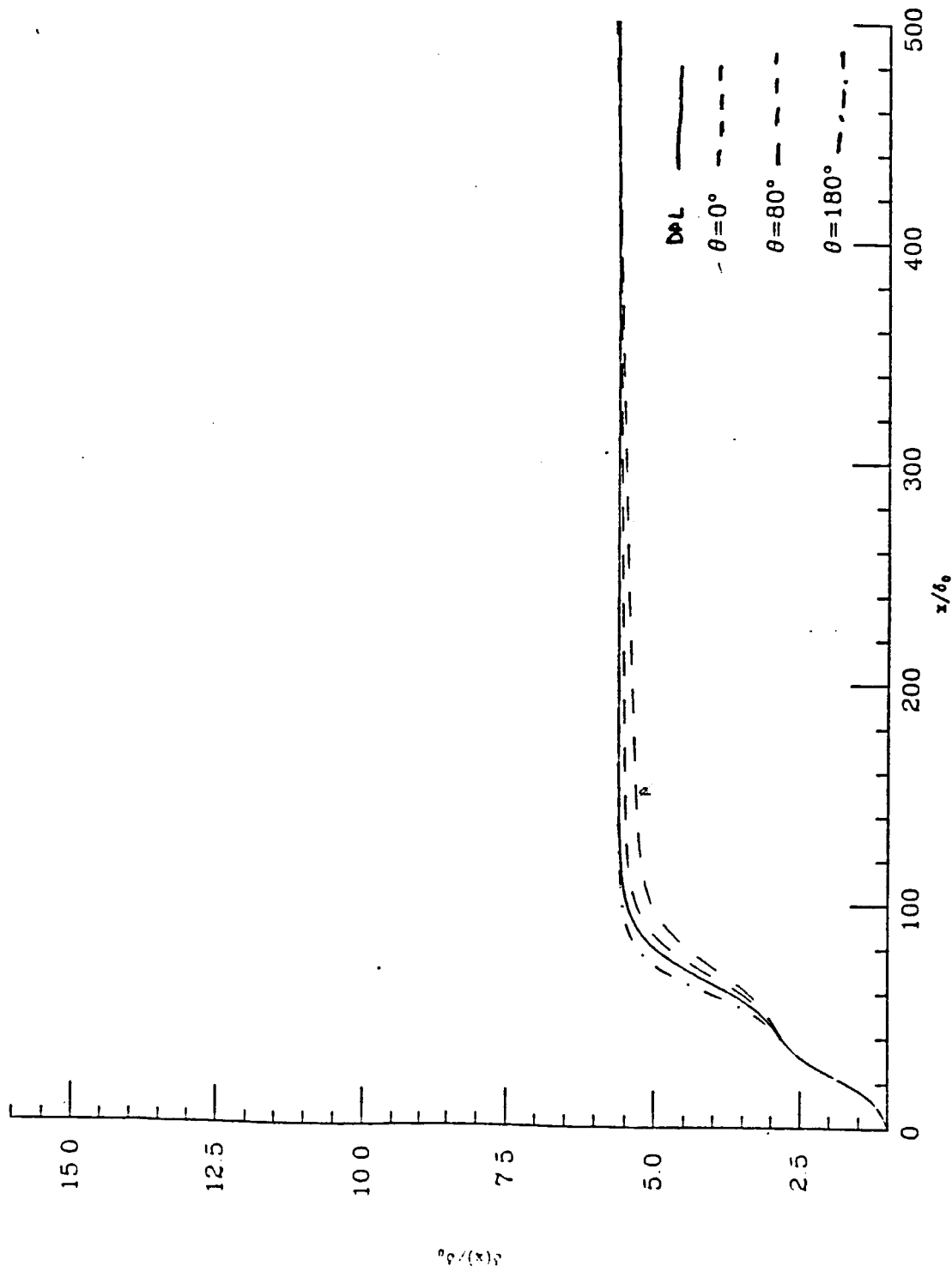


FIG 7b

not
heavy

$\beta_0 = .18, E_1(0) = .12 \cdot 10^{-4}, E_2(0) = .68 \cdot 10^{-4}, Re_0 = 71$

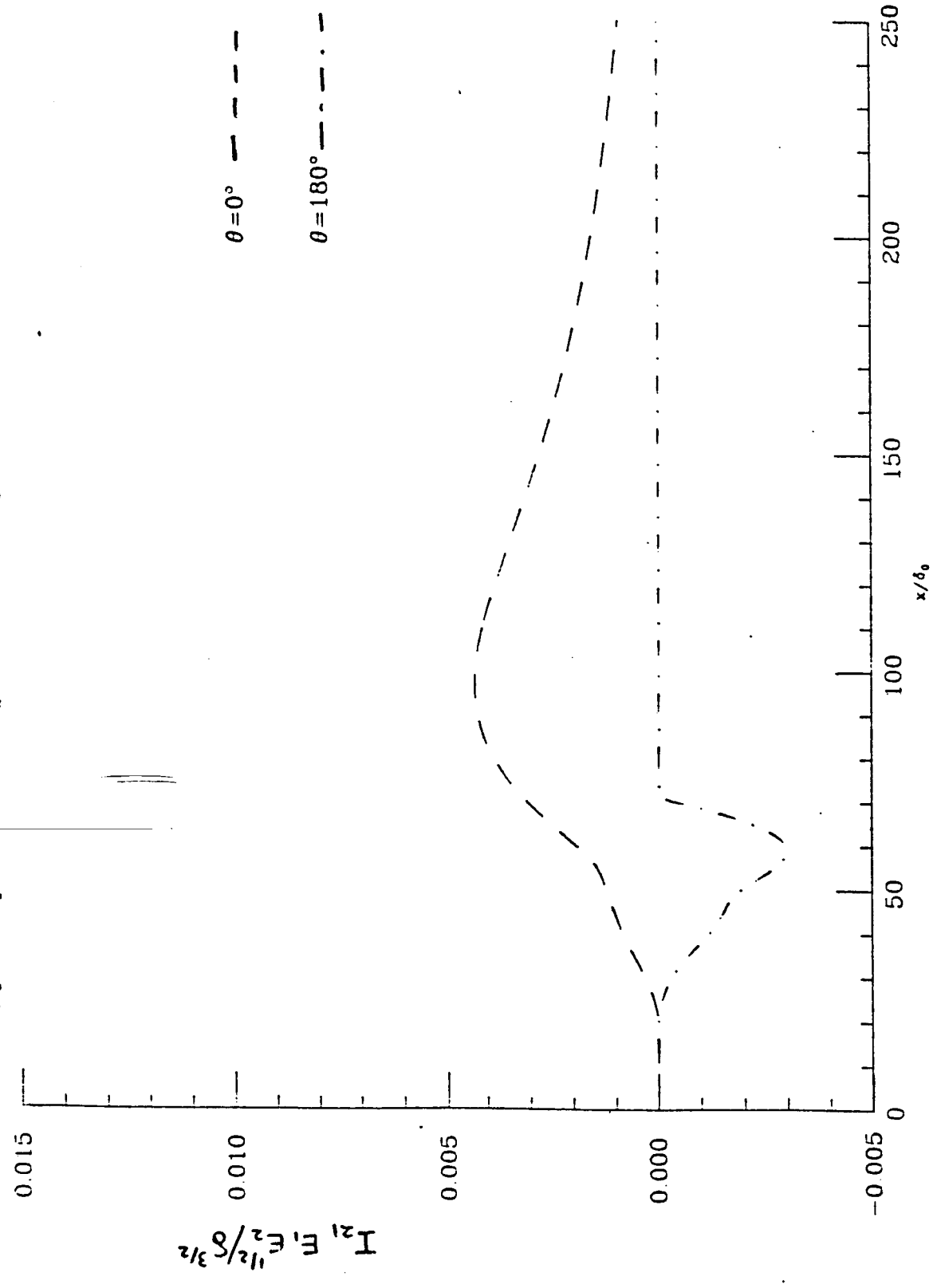


FIG 7C

11-1-1964

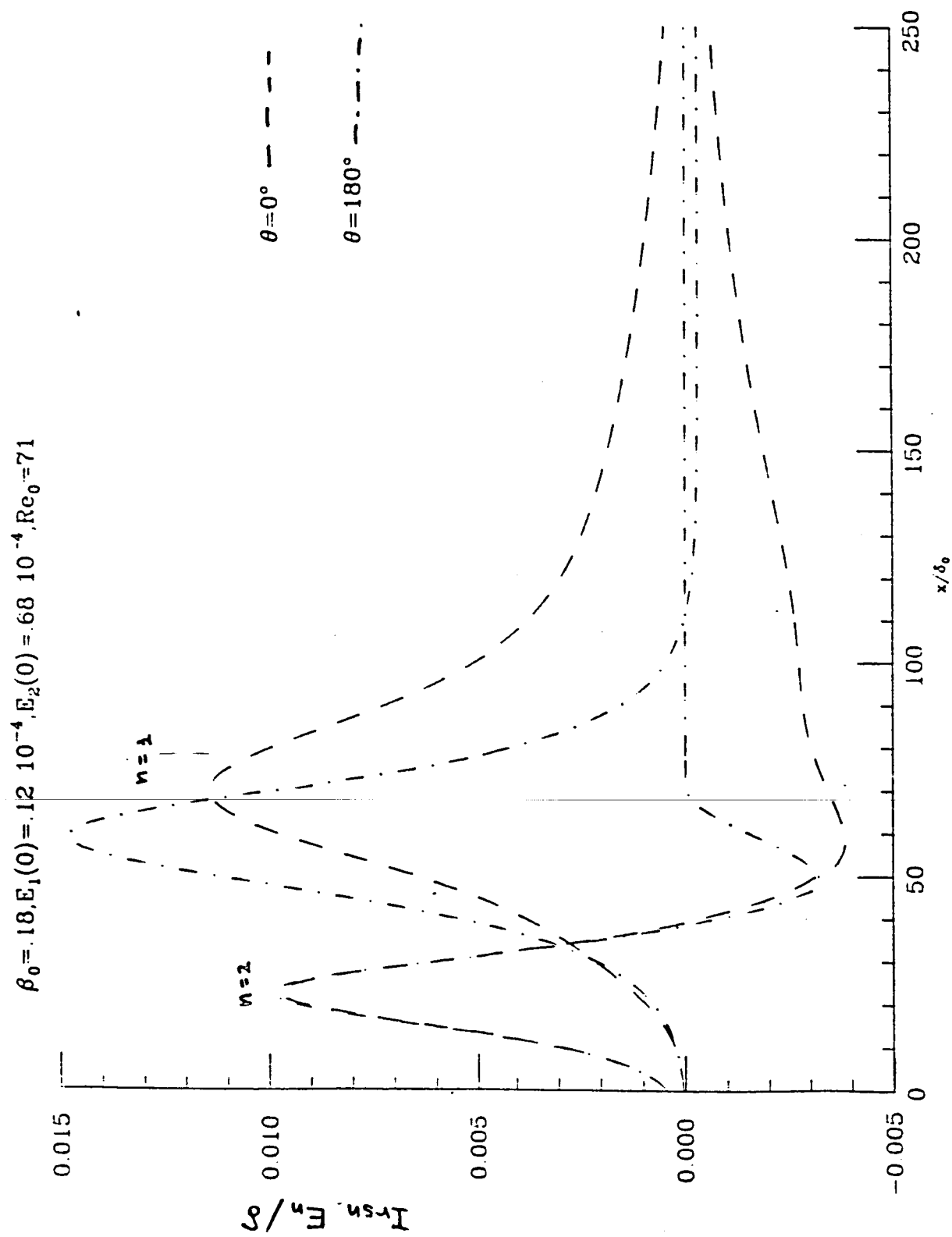


FIG 7d

$\theta=0^\circ, E_1(0)=.12, 10^{-4}, E_2(0)=.68, 10^{-4}, Re_0=71$

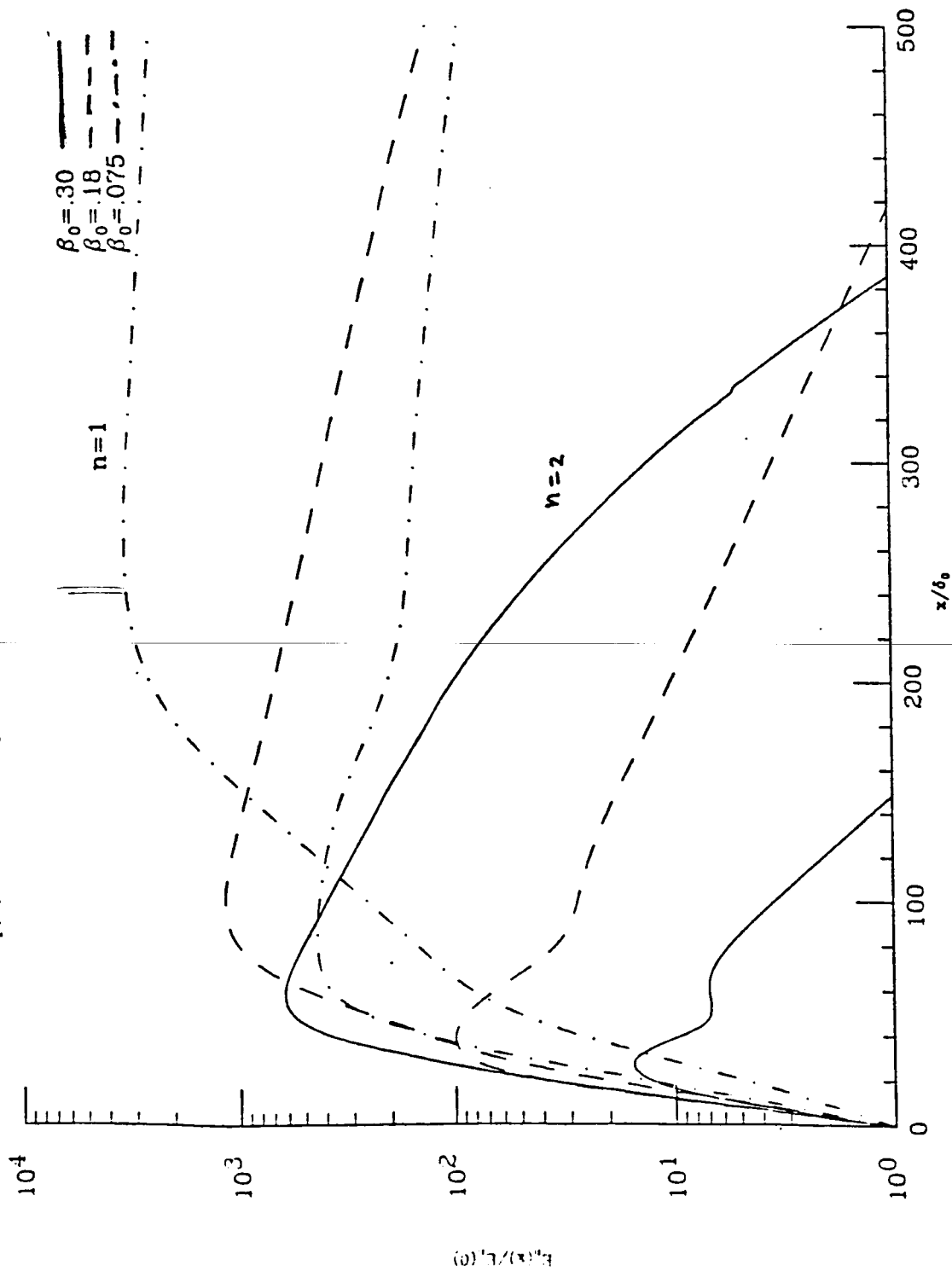


FIG-8a

$\theta = 0^\circ, E_1(0) = .12 \cdot 10^{-4}, E_0(0) = .68 \cdot 10^{-4}, Re_0 = 71$

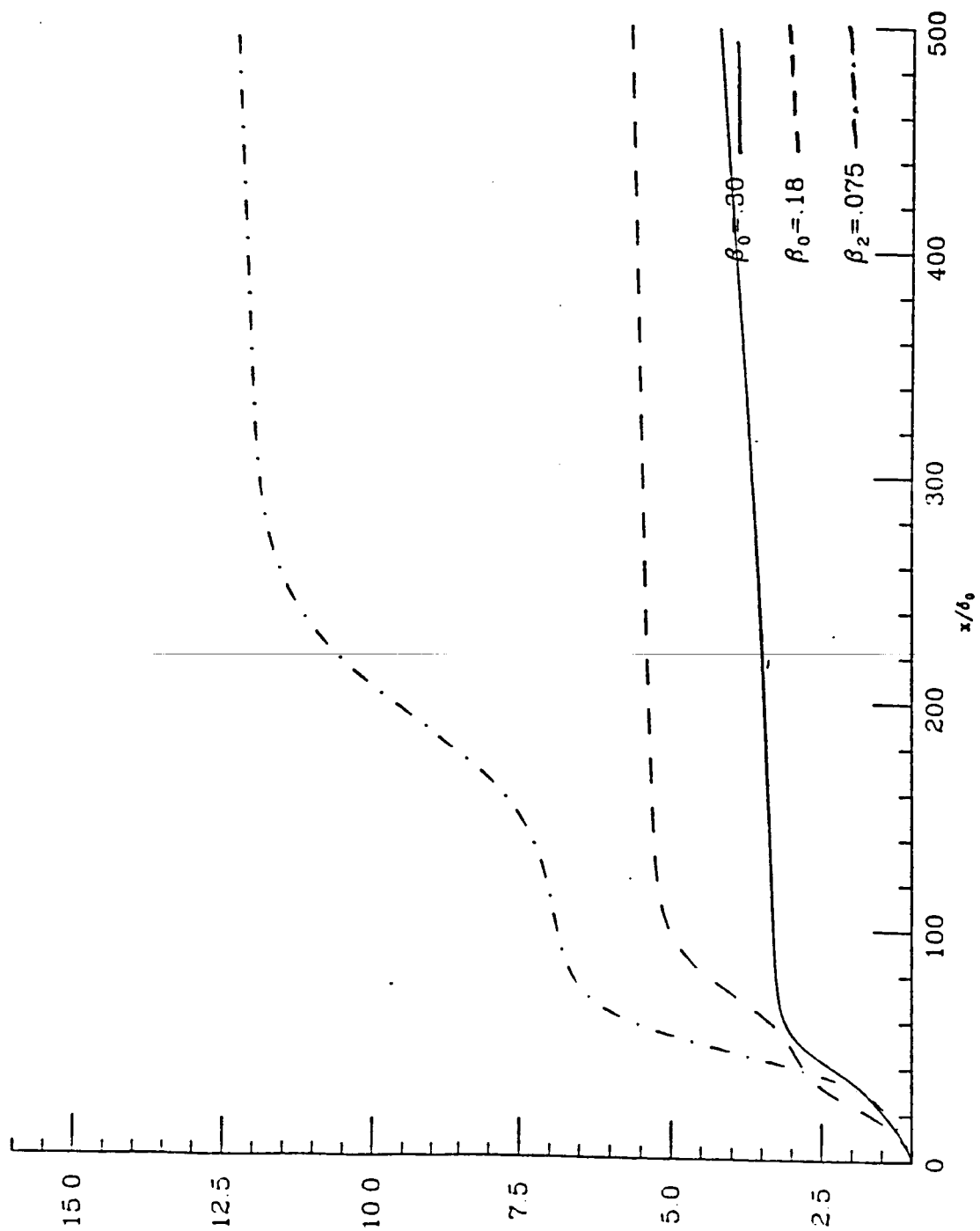


FIG 86

$\theta = 0^\circ, E_2(0) = .68 \cdot 10^{-4}, \beta_0 = .075, Re_0 = 71$

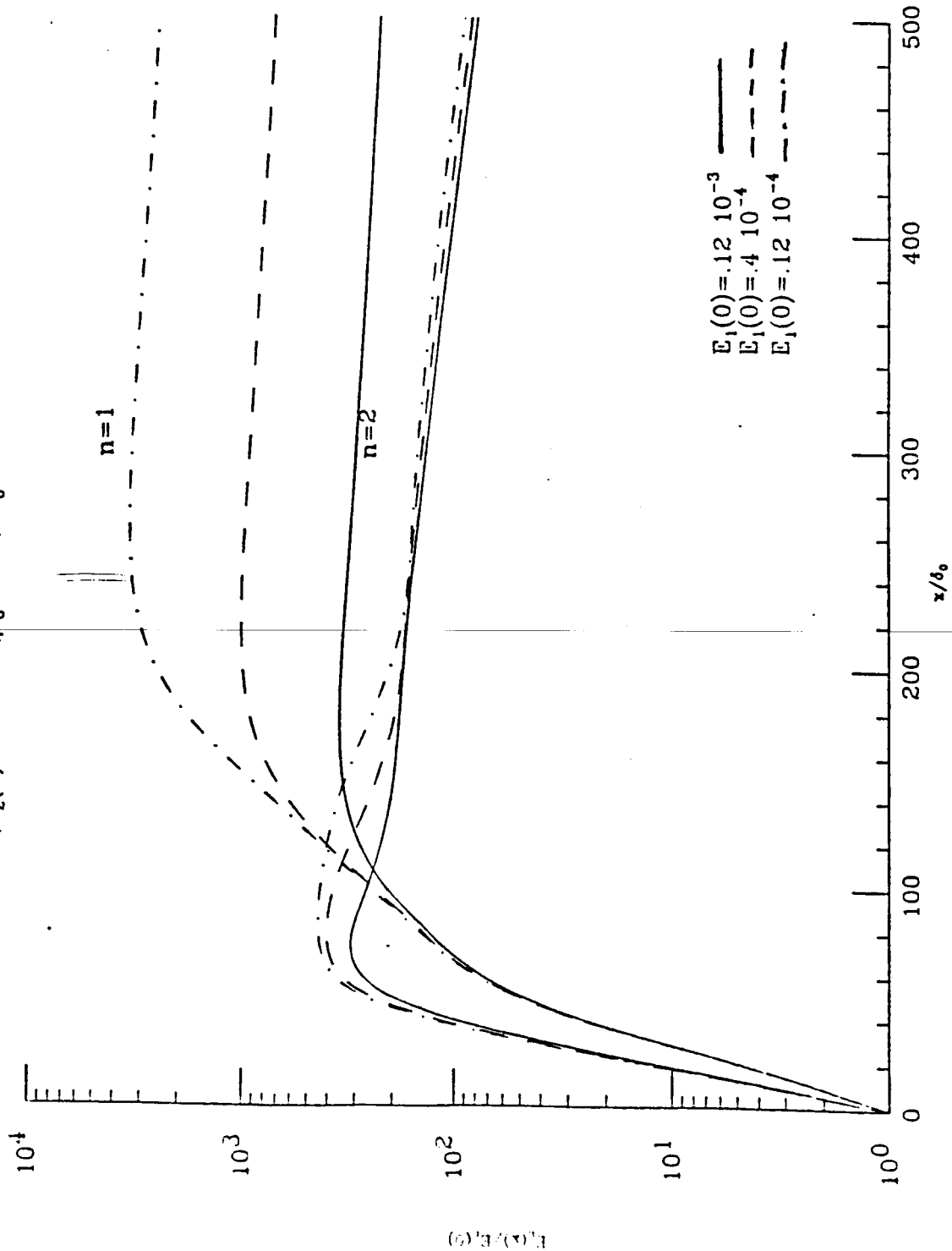


FIG 9a

$\theta = 0^\circ, E_2(0) = .68 \cdot 10^{-4}, \beta_0 = .075, Re_0 = 71$

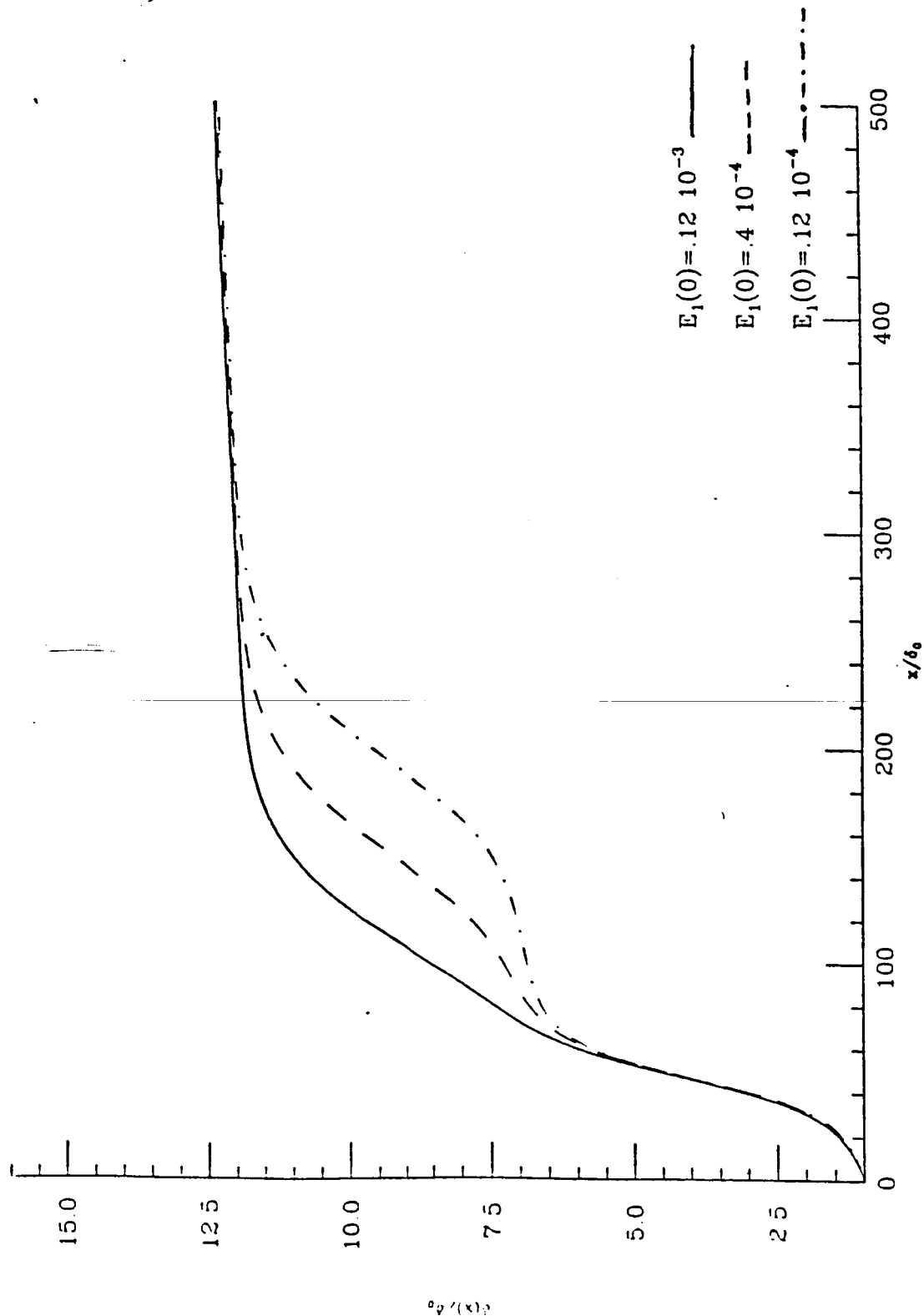


FIG 9b

$\beta_0 = .075, E_2(0) = .68 \cdot 10^{-4}, \theta = 0^\circ, Re_0 = 71$

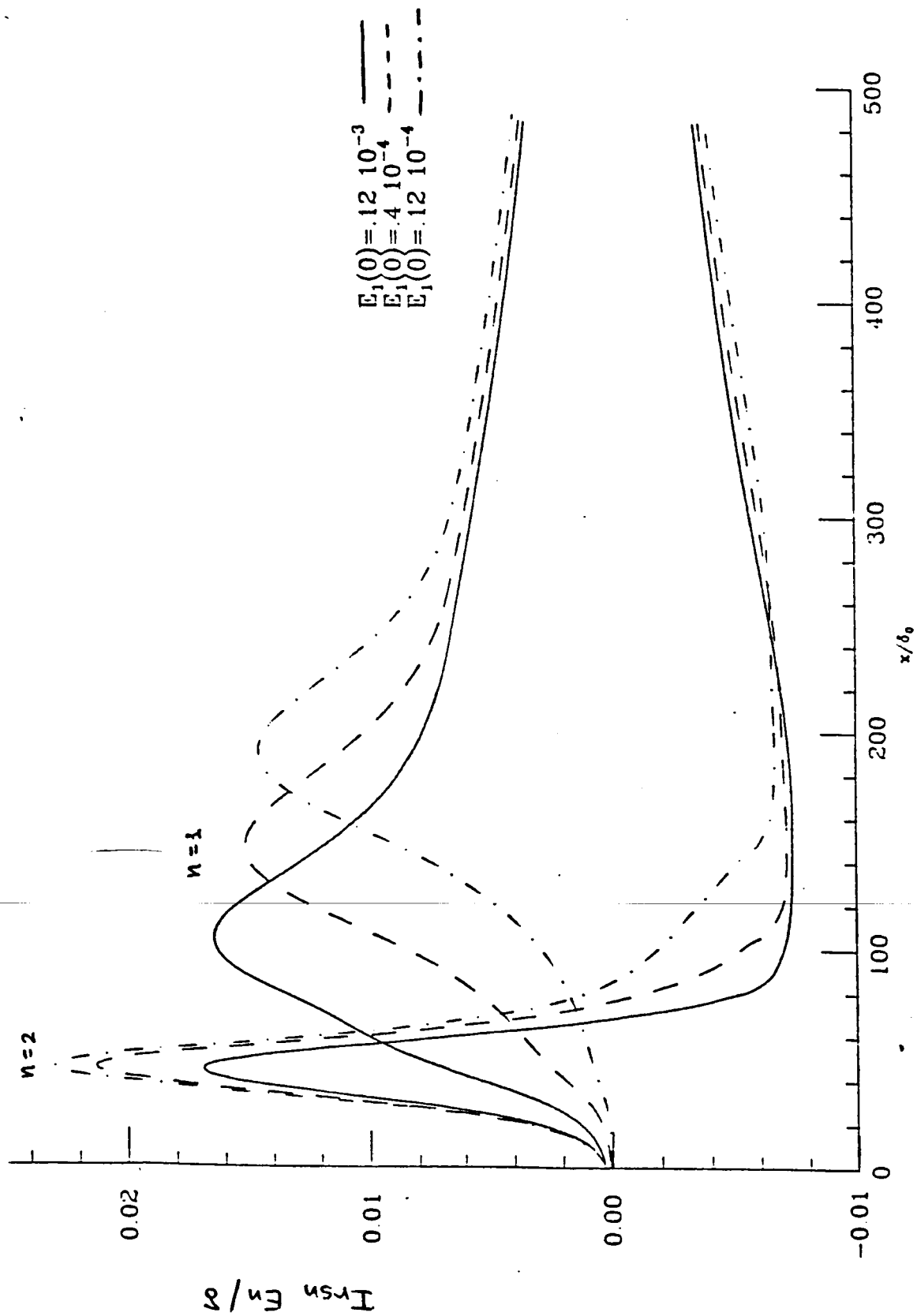


FIG 9c

$\beta_0 = .075, E_2(0) = .68 \cdot 10^{-4}, \theta = 0^\circ, Re_0 = 71$

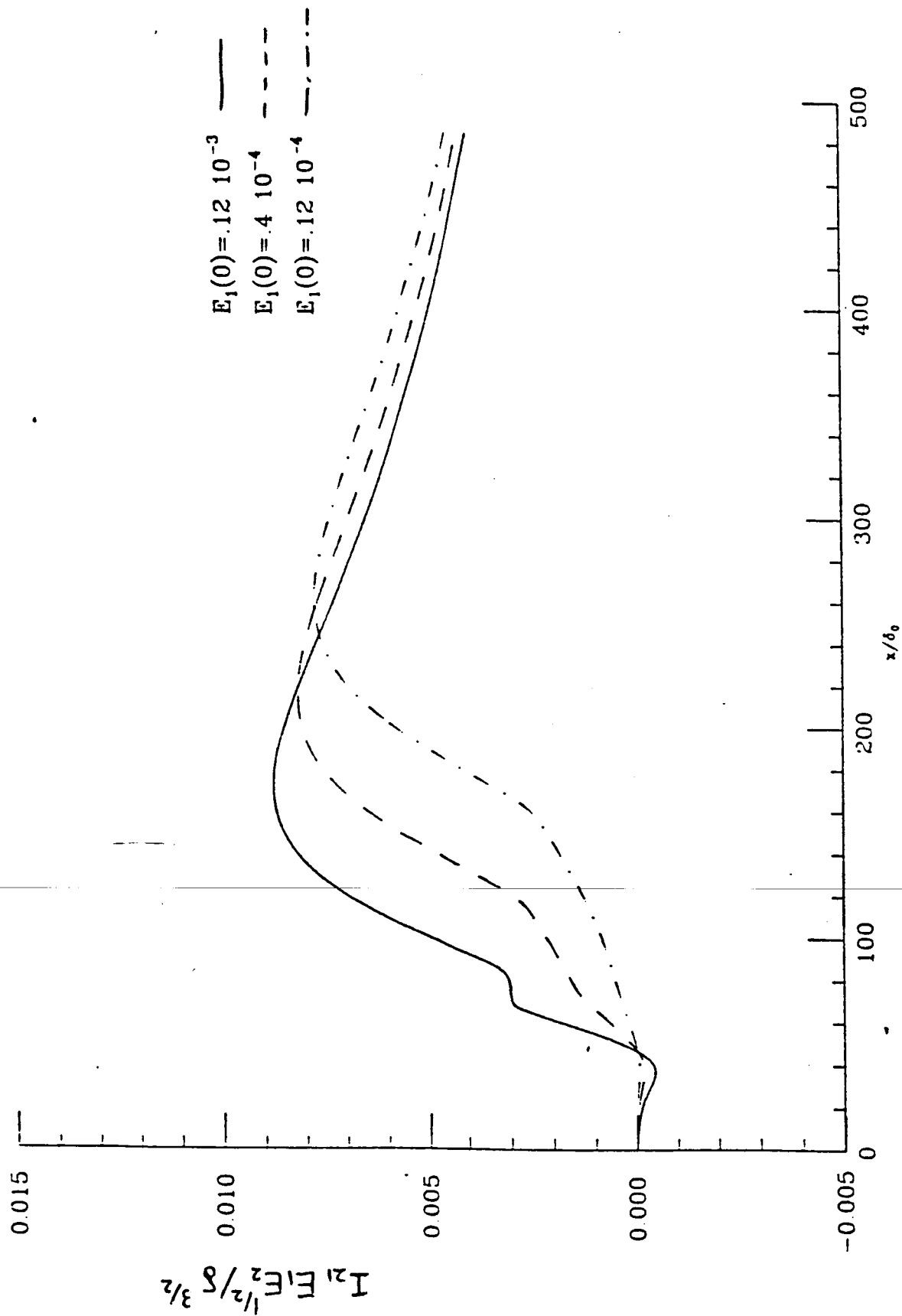


FIG 9d

$\theta=0^\circ, E_1(0)=.12 \cdot 10^{-4}, \beta_0=.075, Re_0=71$

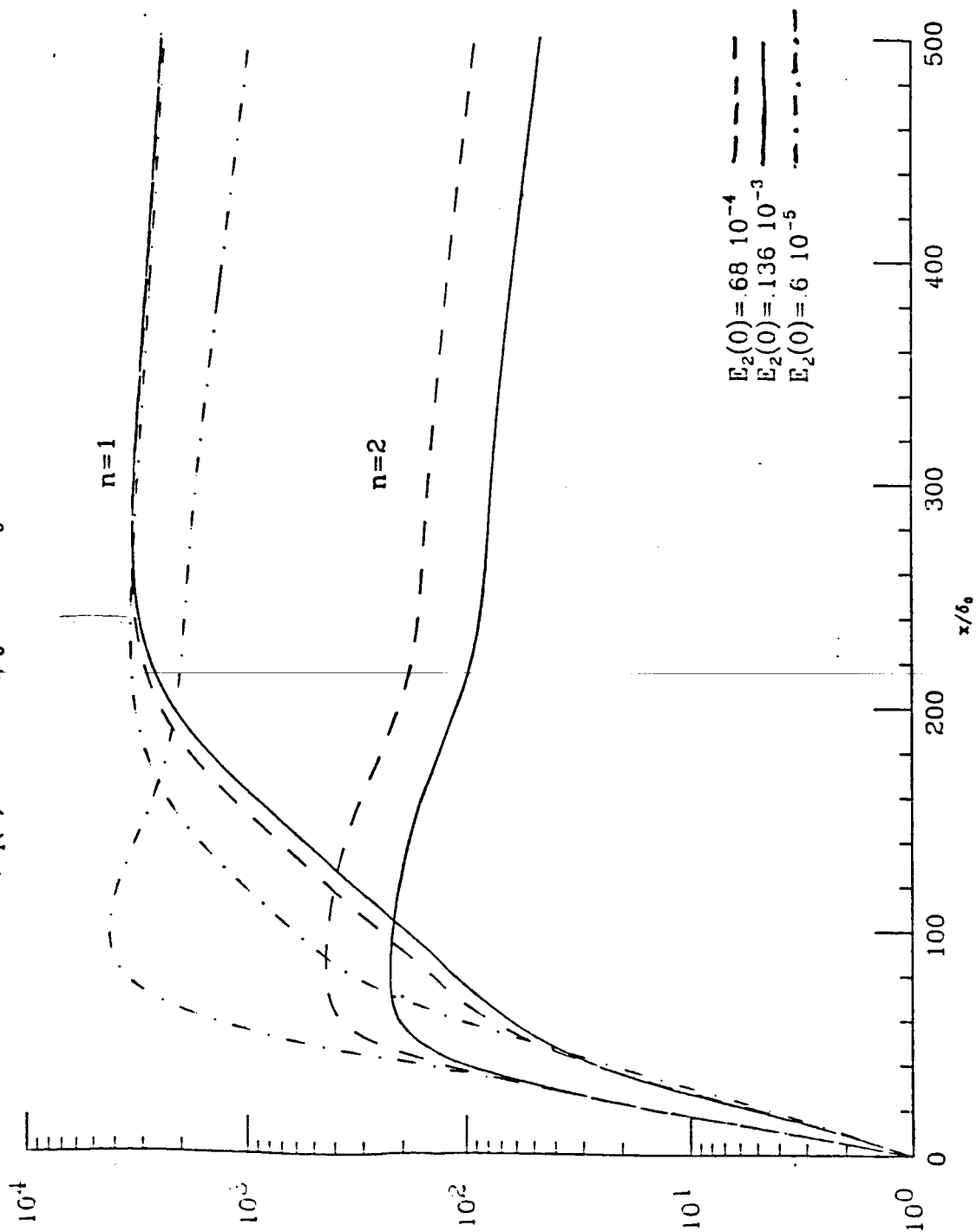


FIG 10a

$\theta = 0^\circ, E_1(0) = .12 \cdot 10^{-4}, \beta_0 = .075, Re_0 = 71$

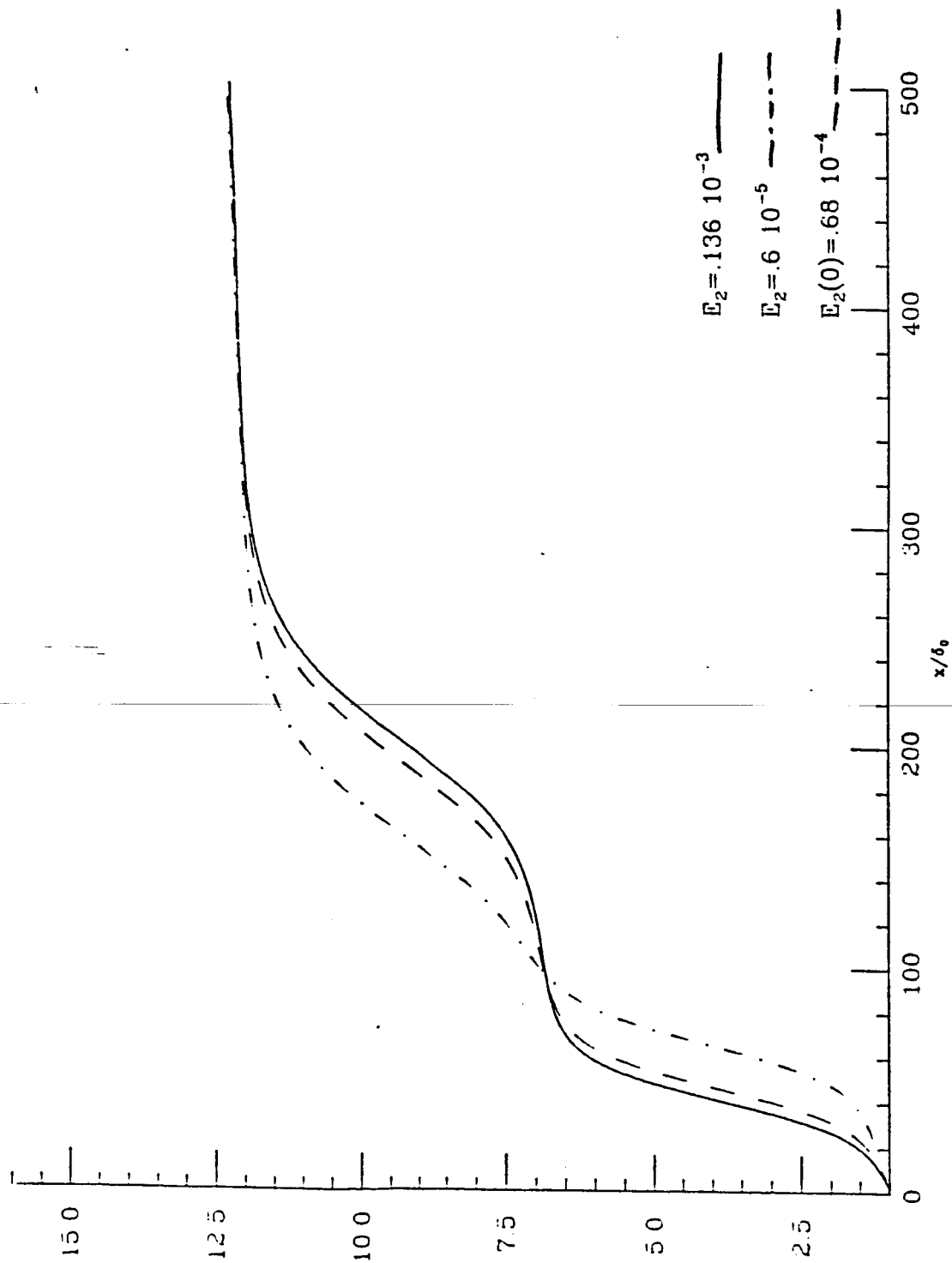


FIG-10b

$$\beta_0 = .075, E_1(0) = .12 \cdot 10^{-4}, \theta = 0^\circ, Re_0 = 71$$

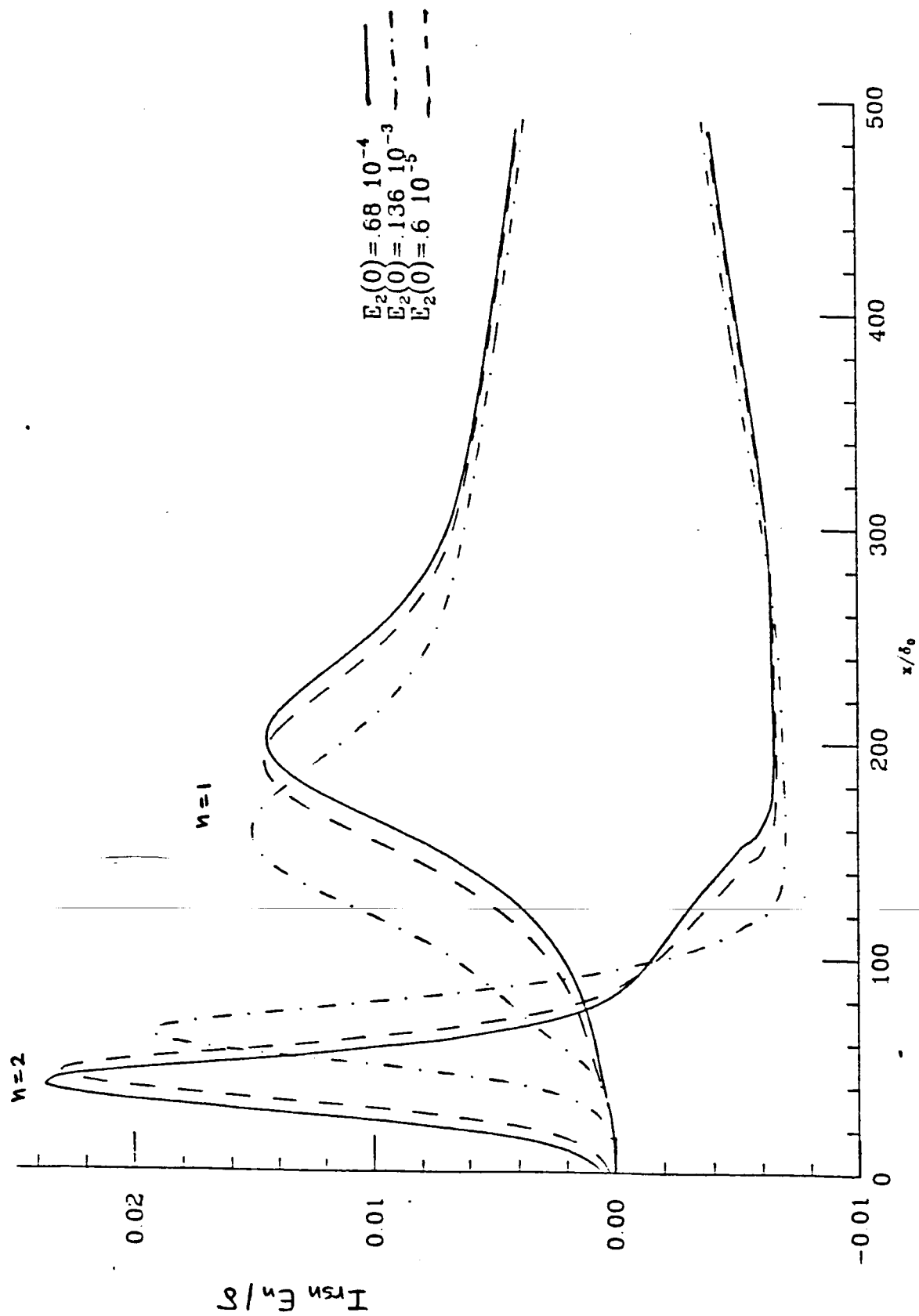


FIG 10c

$\beta_0 = .075, E_1(0) = .12 \cdot 10^{-4}, \theta = 0^\circ, Re_0 = 71$

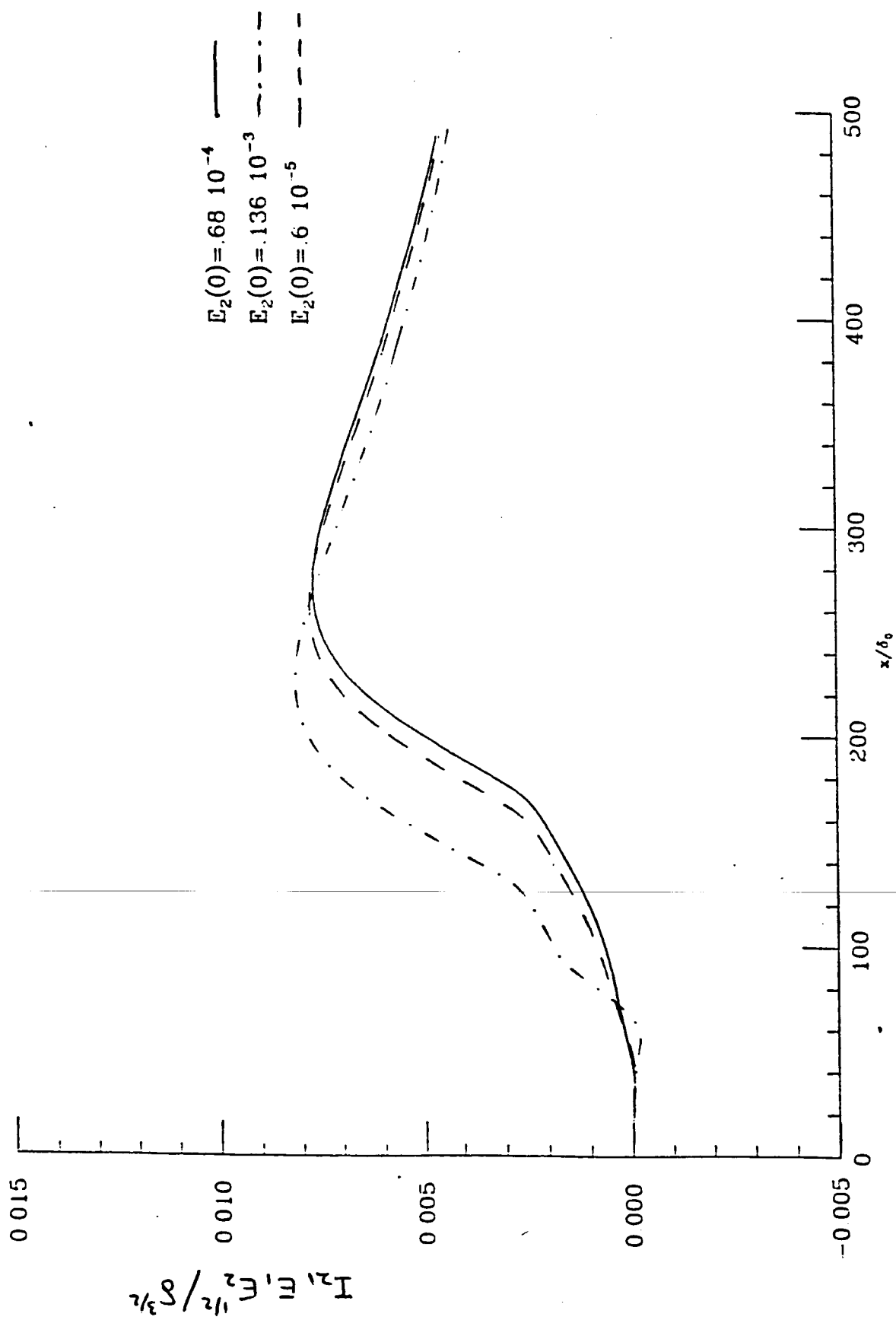


FIG 10d

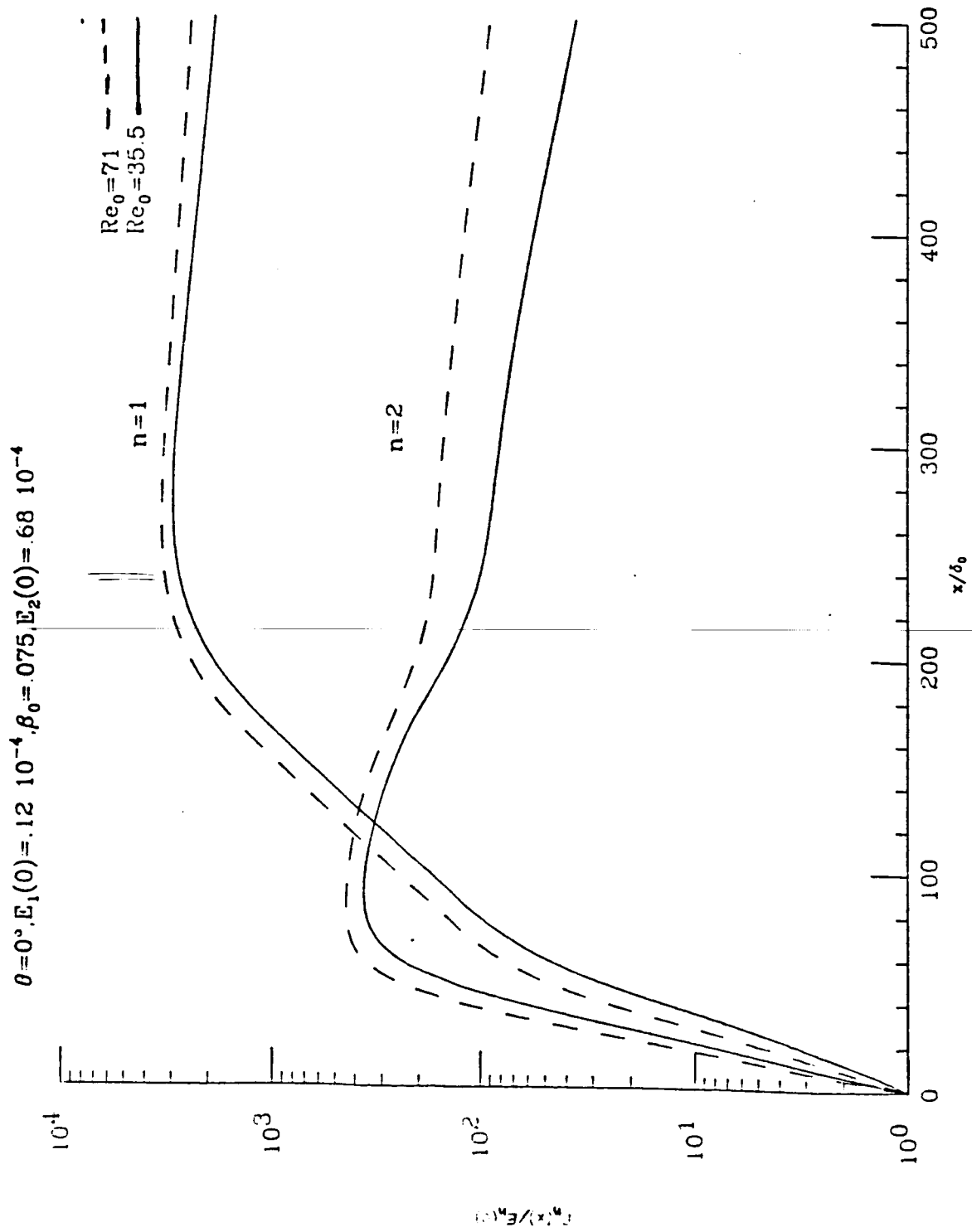


FIG 11a

$$\theta = 0^\circ, E_1(0) = .12 \cdot 10^{-4}, \beta_0 = .075, E_2(0) = .68 \cdot 10^{-4}$$

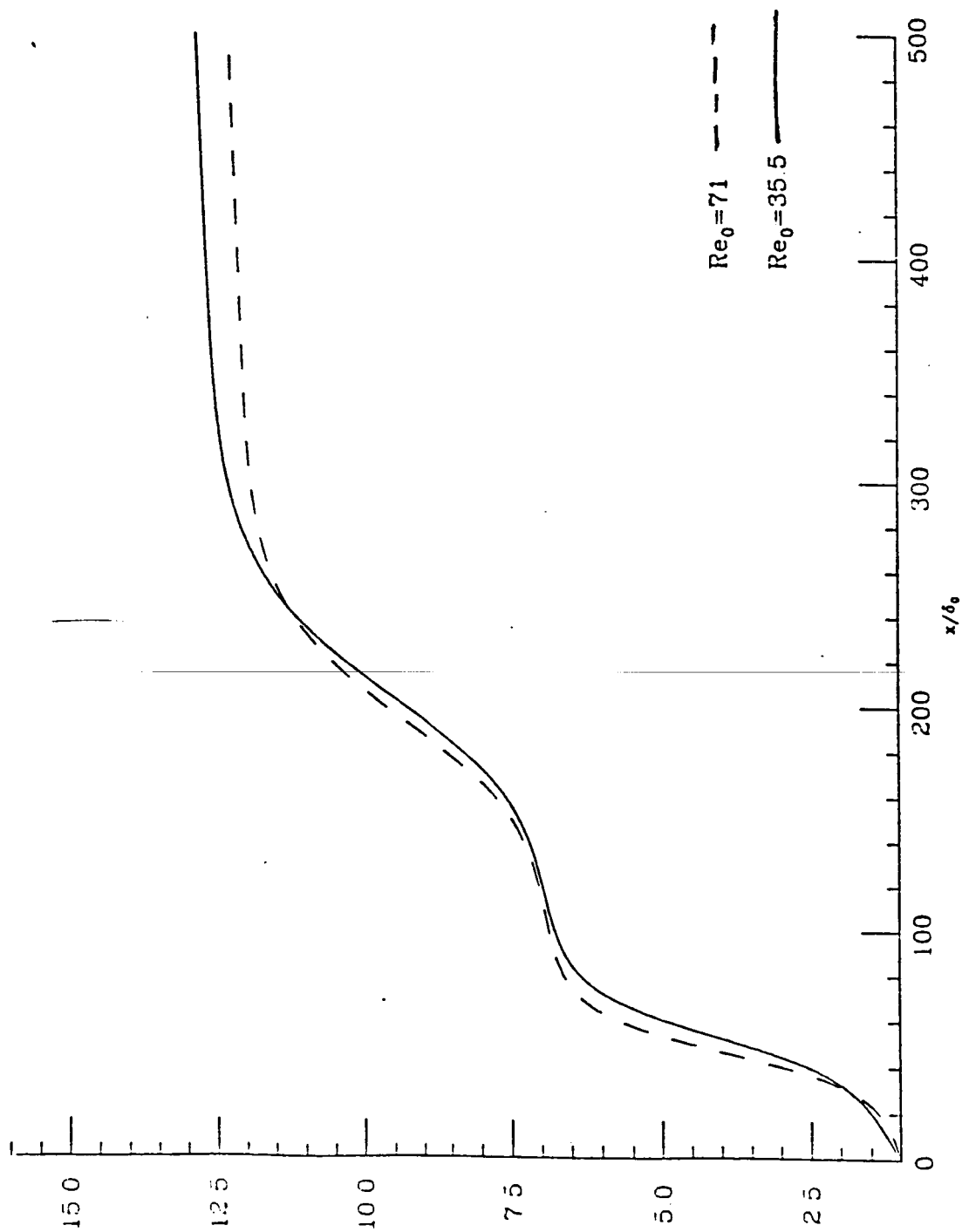


FIG-11b

$$\beta_0 = .260, E_{u1}(0) = .16 \cdot 10^{-4}, E_{u2}(0) = 48 \cdot 10^{-3}, Re_0 = 81$$

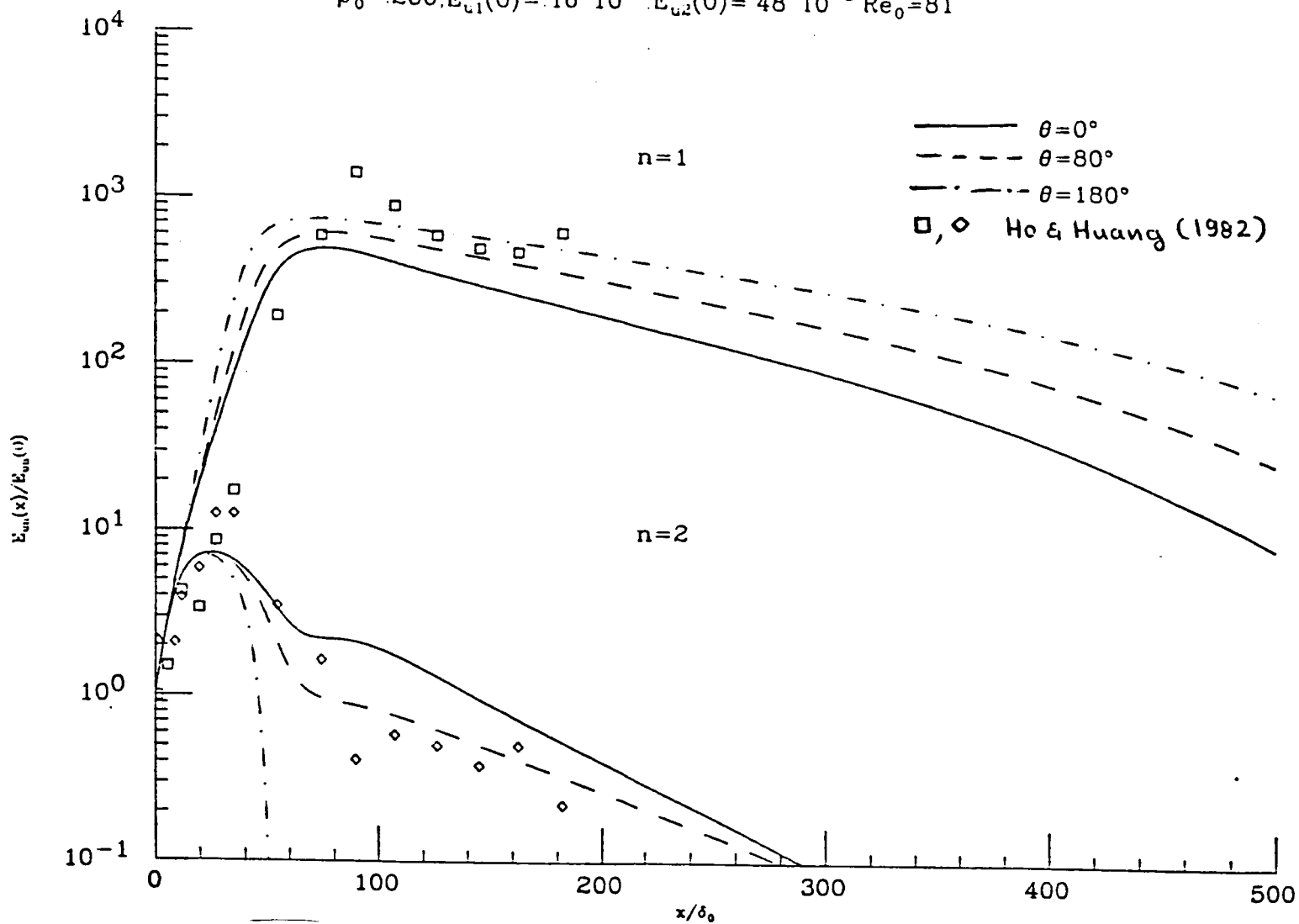


FIG 12a

$$\beta_0 = .260, E_{u1}(0) = .16 \cdot 10^{-4}, E_{u2}(0) = .48 \cdot 10^{-3}, Re_0 = 81$$

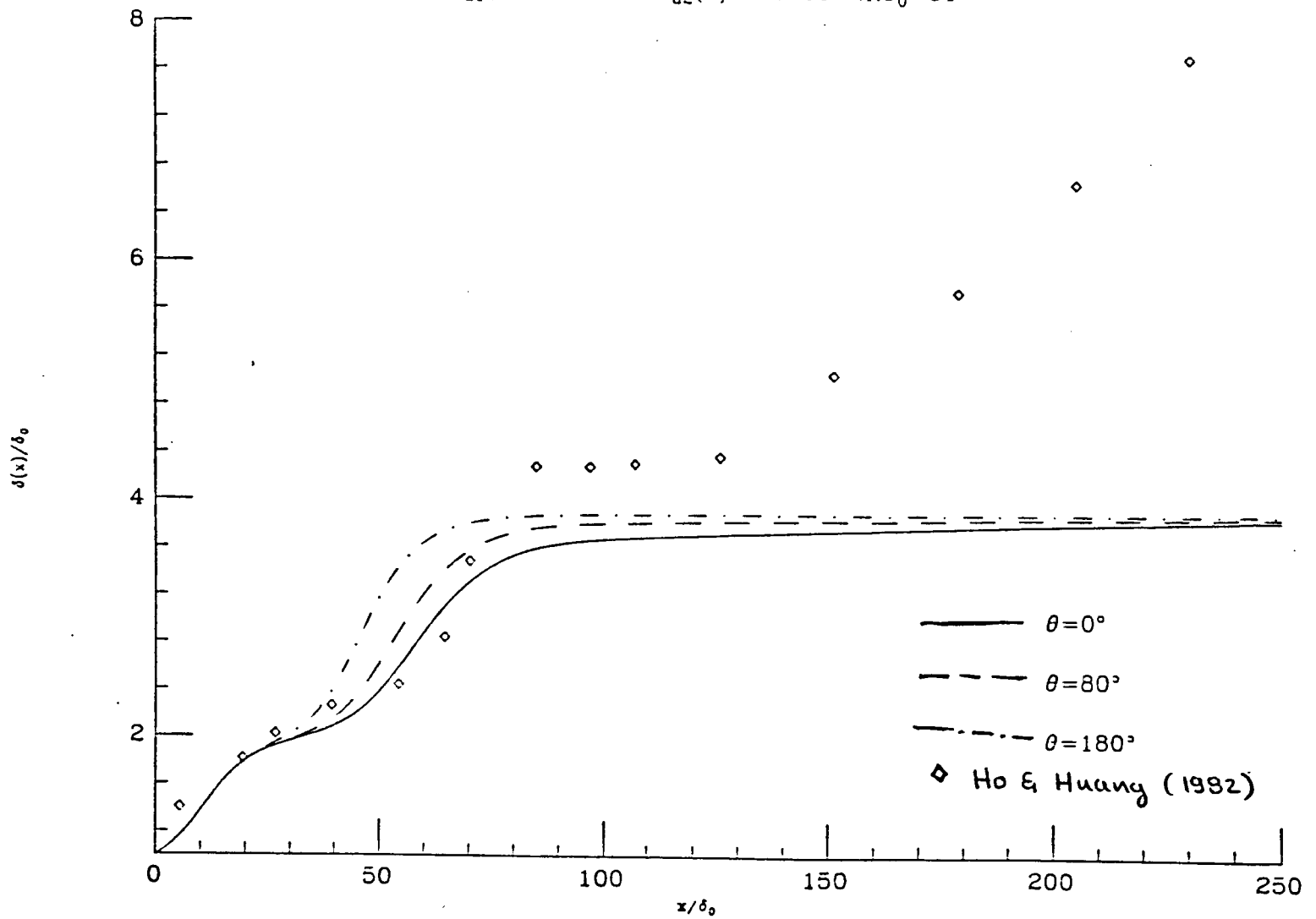


FIG 12b